MISCELLANEOUS PAPER GL-89-17

ESTIMATED GROUND MOTIONS FOR A NEW MADRID EVENT

by

Walter J. Silva, Robert B. Darragh, Robert K. Green
F. Thomas Turcotte

Woodward-Clyde Consultants
500 12th Street, Suite 100
Oakland, California 94607-4014

September 1989
Final Report

Prepared for DEPARTMENT OF THE ARMY
US Army Corps of Engineers
Washington, DC 20314-1000

Under Contract No. DACW39-88-M-0146

Monitored by Geotechnical Laboratory
US Army Engineer Waterways Experiment Station
3909 Halls Ferry Road
Vicksburg, Mississippi 39180-6199

When this report is no longer needed return it to the originator

The findings in this report are not to be construed as an official Department of the Army position unless so designated by other authorized documents.

The contents of this report are not to be used for advertising, publication, or promotional purposes. Citation of trade names does not constitute an official endorsement or approval of the use of such commercial products.

REPORT DOCUMENTATION PAGE

Form Approved OMB No. 0704-0188

1a. REPORT SECURITY CLASSIFICATION Unclassified	1b. RESTRICTIVE MARKINGS
2a. SECURITY CLASSIFICATION AUTHORITY	3. DISTRIBUTION / AVAILABILITY OF REPORT Approved for public release; distribution unlimited.
2b. DECLASSIFICATION / DOWNGRADING SCHEDULE	
4. PERFORMING ORGANIZATION REPORT NUMBER(S)	5. MONITORING ORGANIZATION REPORT NUMBER(S) Miscellaneous Paper GL-89-17
6a. NAME OF PERFORMING ORGANIZATION Woodward-Clyde Consultants 6b. OFFICE SYMBOL (If applicable)	7a. NAME OF MONITORING ORGANIZATION USAEWES Geotechnical Laboratory
6c. ADDRESS (City, State, and ZIP Code) 500 12th Street, Suite 100 Oakland, CA 94607-4014	7b. ADDRESS (City, State, and ZIP Code) 3909 Halls Ferry Road Vicksburg, MS 39180-6199
8a. NAME OF FUNDING / SPONSORING ORGANIZATION US Army Corps of Engineers 8b. OFFICE SYMBOL (If applicable)	9. PROCUREMENT INSTRUMENT IDENTIFICATION NUMBER Contract No. DACW39-88-M-0145
8c. ADDRESS (City, State, and ZIP Code) Washington, DC 20314-1000	10. SOURCE OF FUNDING NUMBERS PROGRAM ELEMENT NO. / PROJECT NO. / TASK NO. / WORK UNIT ACCESSION NO.
11. TITLE (Include Security Classification) Estimated Ground Motions for a New Madrid Event	
12. PERSONAL AUTHOR(S) Silva, Walter, J.; Darragh, Robert B.; Green, Robert K.; Turcotte, F. Thomas	
13a. TYPE OF REPORT Final report 13b. TIME COVERED FROM _____ TO _____	14. DATE OF REPORT (Year, Month, Day) September 1989 15. PAGE COUNT 90
16. SUPPLEMENTARY NOTATION Available from National Technical Information Service, 5285 Port Royal Road, Springfield, VA 22161.	
17. COSATI CODES FIELD / GROUP / SUB-GROUP	18. SUBJECT TERMS (Continue on reverse if necessary and identify by block number) Earthquake, New Madrid, Ground motions, Response spectra

19. ABSTRACT (Continue on reverse if necessary and identify by block number)

The band-limited-white-noise ground motion model coupled with random vibration theory employed in the WES-RASCAL computer program has been used to predict response spectral shapes for earthquakes in both eastern and western North America, and to generate synthetic time histories of ground motion. When this method is applied to the postulated maximum magnitude New Madrid event at close distances, the calculated peak acceleration is about 1.6g for hard rock outcrop motion. Extrapolations of published attenuation relationships yieid similar values, but are beyond the range of the applicability of the relationships due to a lack of strong motion data for large intraplate events at very close distances to the rupture surface. Realistic appearing synthetic acceleration, velocity, and displacement time histories were generated by combining the Fourier amplitude spectrum predicted by the band-limited-white-noise model with the Fourier phase spectrum from ground motion recorded above the source area of the 19 September 1985 Michoacan, Mexico earthquake.

(Continued)

20. DISTRIBUTION / AVAILABILITY OF ABSTRACT ☒ UNCLASSIFIED/UNLIMITED ☐ SAME AS RPT ☐ DTIC USERS	21. ABSTRACT SECURITY CLASSIFICATION Unclassified
22a. NAME OF RESPONSIBLE INDIVIDUAL	22b. TELEPHONE (Include Area Code) / 22c. OFFICE SYMBOL

19. ABSTRACT (Continued).

The effects of a generic deep soil profile, appropriate for the central United States, upon the computed outcrop motion are examined. Both linear and equivalent-linear analyses are performed using a frequency domain wave propagation code. Response is computed for different models of the variation of shear-wave damping with strain. Results indicate that the strain dependency of the shear-wave damping is a controlling factor of the computed response.

PREFACE

This report was prepared by Dr. Walter J. Silva of Woodward-Clyde Consultants, Oakland, California, under Contract No. DACW39-88-M-0145. Dr. Robert B. Darragh, Mr. Robert K. Green, and Dr. F. Thomas Turcotte contributed to the study. Accelerograms from the Guerrero accelerograph array were made available by the Institute of Geophysics and Planetary Physics of the University of California, San Diego and the Instituto de Ingenieria at the Universidad National Autonoma de Mexico, Mexico City.

This study was performed under the guidance of Dr. Ellis L. Krinitzsky, Earthquake Engineering and Geosciences Division (EEGD), Geotechnical Laboratory (GL), US Army Engineer Waterways Experiment Station (WES). The work is part of an ongoing investigation in the Civil Works R&D Program, Earthquake Hazard Evaluations for Engineering Sites. General supervision was by Dr. A. G. Franklin, Chief, EEGD, and Dr. W. F. Marcuson III, Chief, GL.

COL Larry B. Fulton, EN, is Commander and Director of WES. Dr. Robert W. Whalin is Technical Director.

TABLE OF CONTENTS

TABLE OF CONTENTS (concluded)

ESTIMATED GROUND MOTIONS FOR A NEW MADRID EVENT

PART I: INTRODUCTION

Purpose

1. The purpose of this study is to provide estimates of the expected ground motion on competent rock at zero epicentral distance due to a maximum magnitude New Madrid earthquake. Competent rock is defined, for purposes of this study, as rock with a shear wave velocity of 3.5 km/sec. The primary objective is to provide values for peak ground acceleration and response spectral shape (five percent response spectral acceleration divided by peak acceleration). In addition, another goal of this study is to provide a time history consistent with these ground motion parameters.

2. In order to illustrate the effects of a deep soil column, the predicted outcrop motion is propagated through a 500-ft-thick generic sand profile. To demonstrate differences in response between a linear analysis and a nonlinear (through equivalent-linear) analysis, predicted absolute acceleration spectra as well as synthetic acceleration time histories are presented for different assumptions of the shear strain dependency of material damping.

3. It is important to state that the results of this study are intended to demonstrate the predictions using a single analysis method, and are not intended for use in the design of specific structures.

Method

4. The estimates of the ground motion parameters are made using a band-limited-white-noise (BLWN) ground motion model as described by Boore and Atkinson (1987). This model uses the stochastic, constant

stress parameter ground motion model (Hanks, 1979; McGuire and Hanks, 1980; Hanks and McGuire, 1981; Boore, 1983, 1986a; McGuire and others, 1984; Atkinson, 1984; and Boore and Atkinson, 1987) coupled with a simple single corner frequency - omega square source model (Brune, 1970, 1971). Random vibration theory (RVT) is used to relate the root mean square (RMS) values of acceleration, velocity, and oscillator response computed from the power spectra to the corresponding expected peak time domain values. The ground motion model is described in more detail in Part III.

5. Acceleration, velocity, and displacement time histories are developed by combining the Fourier amplitude spectrum from the BLWN model with the phase spectrum of a recorded accelerogram to produce a synthetic time history (Silva and Lee, 1987).

PART II: NEW MADRID EVENT

Historical Perspective

6. A sequence of major earthquakes occurred in the central Mississippi Valley during the winter of 1811-12 that have become known as the New Madrid earthquake(s). The first two earthquakes occurred on December 16, 1811 at 2:15 a.m. and 8:15 a.m. and were followed by major earthquakes on January 23, 1812 at 9:00 a.m. and again on February 7, 1812 at 3:45 a.m. (Street, 1980).

7. At the time of these events, the country west of the Mississippi River was still unsettled except for isolated homesteads. A few cities and towns such as New Madrid were beginning to develop along the Mississippi River. Consequently, descriptions of the damage and destruction from the epicentral region west of the river are incomplete. Nevertheless, the earthquakes were so widely felt across most of the eastern United States that Nuttli (1973b) was able to compile the available descriptive information and assign magnitudes and probable epicentral locations to the main events.

8. Nuttli (1973b) placed the epicenter of the 8:15 a.m. earthquake on December 16, 1811 in northeastern Arkansas near the southern end of the lake formed by the St. Francis river. The epicenter of the February 7, 1812 earthquake was considered to be very near New Madrid, Missouri which was completely destroyed during the earthquake.

9. The strong ground shaking in the epicentral region was accompanied by the opening of large fissures, sand blows, and changes in ground elevation (lines of sight). The vertical changes in elevation were significant: large tracts of land sank, with water subsequently standing to depths of 4 or 5 feet; former lakes were drained, presumably because they were elevated; and the town of New Madrid was lowered from

its original height of 25 feet above river level to only 12 feet above river level following the earthquakes. The zones of surface deformation were sufficiently localized that in at least one case, temporary rapids were formed in the Mississippi River, north of New Madrid. There is no evidence, however, that the faulting extended to the surface.

10. Modern seismographic network coverage of the central Mississippi River Valley has greatly enhanced our understanding of the earthquake activity in this region as revealed by the nature and location of the frequently recorded, smaller magnitude events.

11. These events show that the New Madrid seismic zone consists of three primary segments (Figure 1). The longest segment extends from near Marked Tree, Arkansas to about 20 km northwest of Dyersburg, Tennessee where it terminates against the central segment. This southern segment is approximately 125 km in length along a N50°E trend. A central segment, near the crest of the Pascola Arch, trends roughly N20°W for a distance of about 60 km to a location west of New Madrid, Missouri. The northern segment, approximately 85 km in length, extends N40°E from its juncture with the central segment near New Madrid, to the vicinity of Cairo, Illinois (Stauder et al., 1976, Nuttli, 1983, Mento et al., 1986).

12. The December 16, 1811 earthquake was believed to have occurred near the middle of the southern segment and ruptured the northern half of that segment. Two large aftershocks within the first 12 hours are thought to have ruptured the remainder of the southern segment. The January 23, 1812 earthquake apparently ruptured the entire length of the central segment, and the February 7, 1812 earthquake the entire length of the northern segment (Nuttli, 1983).

13. Focal mechanisms of recent activity along these trends show oblique right lateral motion on northerly to northeast-trending faults and left lateral motion on westerly to northwest-trending faults. The motion on north or northeast fault planes has a plunge of about 30°. Both reverse and normal faulting has been observed (Herrmann and Canas, 1978).

Source Characteristics

Magnitude, Moment, Stress Drop

14. Nuttli (1983) estimated the source parameters of the main earthquakes of the 1811-1812 series as follows:

Date	Magnitude (m_b)	Magnitude (M_s)	Moment, Mo (dyne-cm)	Length (km)	Width (km)	Stress Drop, σ (bars)
16 Dec 1811	7.2	8.5	4.0×10^{27}	60	35	100
23 Jan 1812	7.1	8.4	2.5×10^{27}	50	30	90
07 Feb 1812	7.4	8.8	7.9×10^{27}	70	40	120

Previously Herrmann et al., (1978) estimated a range of moment from 4.4×10^{26} to 6.8×10^{27} dyne-cm for the 16 December event and considered 6.3×10^{27} dyne-cm an average value. Because the three main shocks were so similar in size, they considered the total moment to be 6.3×10^{27} dyne-cm and modeled the fault as a plane trending N50°E, dipping 65°W, 15 km in width, 120 km in length with an average displacement of 10 m ($\mu = 3.53 \times 10^{11}$ dynes/ cm^2) for an event with $M_s = 8.0$, an average stress drop of 60 bars and an apparent stress drop of 30 bars. This model was used in estimating the areal distribution of surface displacement for the series of earthquakes.

15. Anderson (1986b) adopted Nuttli's m_b values for these events, but determined the moments for the 16 Dec 1811, 23 Jan 1812 and 7 Feb 1812 earthquakes to be at 6.6×10^{26}, 4.3×10^{26}, and 1.5×10^{27} dyne-cm, respectively, with a sum of 2.6×10^{27} dyne-cm. Anderson used empirical moment-magnitude relationships rather than fault dimensions and displacement to estimate the seismic moment.

Focal depth

16. The smaller magnitude earthquakes currently recorded are mainly located at depths between 5 and 15 km, but have been observed as deep as 22 km (Herrmann et al., 1978). Nuttli (1981) considered a fault width of 15 km to be appropriate for the entire region. The current activity suggests a depth of 10 km to be a reasonable hypocentral depth for the New Madrid events. Herrmann, Cheng, and Nuttli (1978) modeled the surface deformation with a fault plane at depths between 5.2 and 18.8 km beneath the surface, corresponding to a source at 12 km depth on a fault striking N50°E, with a dip 65° West. Changing the source depth to 9 km brought the top of the rupture plane within 2.2 km of the surface, but failed to alter the surface deformation pattern enough to provide a definitive estimate of the focal depth from the historical observations.

PART III: GROUND MOTION MODEL

17. The band-limited-white-noise (BLWN) ground motion model in which the energy is distributed randomly over the duration of the source has proven remarkably effective in correlating with a wide range of ground motion observations (Toro, 1985; Boore, 1986a). Time-domain measures such as peak acceleration and peak particle velocity, Wood-Anderson magnitude, and short-period P- and S-wave amplitudes, as well as, frequency domain measures such as, relative velocity response and Fourier amplitude spectra have been predicted with reasonable accuracy using the stochastic ground motion model (Boore, 1983; McGuire et al., 1984; Boore, 1986a; Boore and Atkinson, 1987; Toro and McGuire, 1987). The stochastic ground motion model employed here uses an ω-square source model (Brune, 1970, 1971) with a single corner frequency and a constant-stress-parameter (Boore, 1983; Atkinson, 1984). Random vibration theory is used to relate RMS values to peak values of acceleration (Boore, 1983), and oscillator response (Boore and Joyner, 1984; Toro, 1985; Silva and Lee, 1987) computed from the power spectra to expected peak time domain values (Boore, 1983).

The shape of the acceleration spectral density a(f) is given by

$$a(f) = C \frac{f^2}{1+(f/fc)^2} \frac{Mo}{R} P(f) A(f) e^{\left|-\frac{\pi f R}{\beta Q(f)}\right|}$$

where C = constant which contains source region density and shear-wave velocity terms and accounts for the free surface effect, the source radiation pattern, and the partition of energy into two horizontal components.

M_o = seismic moment,

R = hypocentral range,

β = shear wave velocity at the source,

Q(f) = frequency dependent quality factor,

A(f) = near-surface amplification factors (Boore, 1986a),

P(f) = high-frequency truncation filter, and

f_c = source corner frequency.

18. Source scaling is provided by specifying two independent parameters, taken to be seismic moment (M_o) and the high-frequency stress parameter ($\Delta\sigma$). The moment is related to magnitude through the definition of moment magnitude (M_w), by the relation:

$$\log M_o = 1.5\ M_w + 16.1 \text{ (Hanks and Kanamori, 1979)},$$

19. The stress parameter, $\Delta\sigma$ is assumed to be independent of magnitude and is taken to be 50 bars in western North America (WNA) (Boore, 1986a) and 100 bars in eastern North America (ENA) (Toro, 1985; Boore and Atkinson, 1987). The Q(f) models are shown in Table 1 along with the remaining parameters considered to be representative of the WNA and ENA tectonic environments. The near-surface amplification factors (Table 2) that account for the increase in amplitude as the seismic energy travels through lower velocity crustal materials near the surface, are taken from Boore (1986a). Because the near-surface (upper crustal) velocity gradients are smaller in the central and eastern tectonic environments, the factors are applied only in the WNA simulations (Boore and Atkinson, 1987).

20. The Fourier amplitude spectrum given by the equation for a(f) represents the BLWN ground motion model employing a single corner frequency, Brune source spectrum. In order to compute peak time domain

values, peak acceleration and peak ocscillator response, random vibration theory is used to relate RMS computations to peak value estimates. Boore (1983) and Boore and Joyner (1984) contain an excellent development of the RVT methodology as applied to the BLWN ground motion model. The procedure, in general, involves computing the RMS value by integrating the power spectrum from zero frequency to the Nyquist frequency and applying Parsevall's relation. Extreme value theory is then used to estimate the expected ratio of the peak value to the RMS value of a specified duration of the BLWN time history. The duration is generally taken as the inverse of the corner frequency (Boore, 1983).

21. The P(f) filter is an attempt to model the observation that acceleration spectral density appears to fall off rapidly beyond some region-dependent maximum frequency. This observed phenomenon truncates the high frequency portion of the spectrum and is responsible for the band-limited nature of the stochastic model. This spectral fall off has been attributed to near-site attenuation (Hanks, 1982; Anderson and Hough, 1984) or to source processes (Papageorgiou and Aki, 1983) or perhaps to both effects. Two forms have been proposed for this filter: (1) an acausal four-pole low-pass Butterworth filter with a corner frequency given by Hanks' site-dependent f_{max} (Boore, 1983) and (2) a site and distance dependent exponential filter proposed by Anderson and Hough (1984). The form of the Butterworth filter is given by:

$$P(f) = [1 + (f/f_m)^8]^{-1/2}$$

where f_m is taken as f_{max} (Hanks, 1982; Boore, 1983, 1986a).

22. The other form of the P(f) filter, the exponential filter, is given by

$$P(f) = e^{-\pi\kappa f}$$

where kappa (κ) is a site and distance dependent parameter that represents the effect of intrinsic attenuation in propagation through the upper crust. Kappa has been determined for several rock and soil sites representative of WNA (Anderson and Hough, 1984; Anderson, 1986a). For WNA rock sites, a value near 0.02 sec is appropriate (Boore, personal communication, 1988). For ENA, the relationship kappa = $\frac{1}{\pi f_{max}}$ may be used to infer a kappa of 0.008 sec consistent with an ENA f_{max} of 40 Hz (Boore and Atkinson, 1987). This relationship produces response spectra which have peak spectral amplification near the same period for P(f) modeled by kappa or f_{max}. The relationship kappa= $\frac{1}{2\pi f_{max}}$ results in a kappa of 0.004 sec for an f_{max} of 40Hz. For this relationship, the RMS values are nearly equivalent (Toro, personal communication, 1988). For this study kappa=0.006 sec was found to be consistent with response spectral shapes of recorded ground acceleration data in ENA. Figure 2 shows the effects on spectral shapes predicted by the BLWN process for an f_{max} of 40 Hz and a kappa of 0.006 sec compared to the average spectral shape computed from recordings of the m_b 6.4 Nahanni earthquake (note that Nahanni is classified as an ENA event because of its intraplate location and crustal characteristics). The features of the spectral shape computed using the kappa operator differ substantially from those characteristic of the f_{max} operator. As expected, the exponential filter results in a smoother shape for frequencies beyond about 15 Hz. The lower peak accelerations computed using the exponential filter compared to those computed using the Butterworth filter are consistent with the results of Luco (1985) and Boore (1986b).

23. The departure of the predicted spectral shape using an f_{max} of 40 Hz or a kappa of 0.006 sec from the trend shown by the data beyond about 20 Hz suggests a departure from model predictions. However, this overprediction may be an artifact of the recording since the strong motion instruments (SMA-1) all had corner frequencies near 25 Hz. While instrument corrections were performed (Wiechert et al.,

1986), it is notoriously difficult to correct with confidence through an instrument corner unless very accurate phase and amplitude calibrations are available. Thus confidence in the data should not be particularly high for frequencies exceeding 20-25 Hz. The kappa operator appears to give a reasonable representation of the spectral shape computed from recorded data over the bandwidth of interest (1-25 Hz) to critical structures.

PART IV: RESPONSE SPECTRAL CONTENT: MODEL PREDICTIONS AND OBSERVED DATA

24. Strong ground motion observed at rock sites in ENA appears to have different spectral properties than those typical of WNA rock motions.

25. In order to illustrate the differences in spectral content between typical ENA and WNA strong ground motion data from events at similar magnitudes, a form of spectral averaging as well as normalization for different source to receiver distances is required. A convenient measure which approximately normalizes for distance is the spectral amplification (Silva and Green, 1988), defined as response spectral acceleration divided by peak acceleration (Sa/a). Additionally, the technique of averaging response spectral shapes has been used traditionally in the earthquake engineering community as a means of obtaining a statistically significant, as well as reasonably smooth, estimate of the spectral composition expected from earthquakes of a given magnitude and distance range. As such, response spectral shapes are generally familiar and departures can be easily recognized and their significance appreciated. We suggest, however, that spectral ordinates be predicted directly when specifying seismic hazard for a given site. Figure 3 shows average spectral shapes computed from recordings obtained on rock during a Nahanni earthquake (m_b = 6.4, Table 3) compared to an average spectral shape computed from $M_w \approx 6.5$ WNA rock motions (Table 4). The differences in spectral content are significant and indicate that, for the same level of peak acceleration, ENA spectral content is higher than that in the WNA for frequencies greater than approximately 10 Hz.

26. Figures 2 and 4 are a comparison of the RVT 5% response spectral shape with the average and the extremes of the 5% response spectral shapes from recorded data (Mw ≈ 6.5, distance ≈ 25 km) in ENA and WNA, respectively. The RVT estimate of the 5% response spectral

shape matches the average shape closely over the entire range of periods from 0.03 to 4 seconds in Figure 4. In Figure 2, the RVT estimate of the shape matches the average shape reasonably well over the range of periods from 0.05 to 2 seconds. For periods between approximately 0.02 to 0.05 seconds, the RVT spectral magnification is larger than the recorded spectral magnification. This overprediction may again be an artifact of the recording since the strong motion instruments (SMA-1) all had corner frequencies near 25 Hz as discussed in Part III. For the bandwidth (0.5 to 20 Hz), the RVT 5% response spectral shapes are a reasonable representation.

27. Figure 5 is a comparison of the RVT 5% response spectral shape for ENA and WNA parameters (Table 1) with the 5% response spectral shape described in Regulatory Guide 1.60. The shape in Regulatory Guide 1.60 is based on western United States strong motion recording instruments sited on both rock and soil. The inclusion of soil sites raises the shape above the rock RVT shape for periods longer than approximately 0.1 seconds. The RVT 5% response spectral shape predicted for ENA does not match the Regulatory Guide 1.60 shape. At periods less than approximately 0.1 seconds, the Regulatory Guide shape is lower due to the greater amount of high frequency energy in eastern United States ground motions as documented, for example, by a region dependent f_{max} or kappa. At longer periods, the Regulatory Guide shape is higher because it was developed from recordings at both soil and rock sites.

28. Other sources of data also indicate that ENA ground motion recorded at rock or very shallow soil sites is richer in high frequency energy relative to analogous WNA recordings. These include aftershocks of the 1982 Miramichi, New Brunswick event (Cranswick et al., 1985), the 1982 Enola, Arkansas swarm (Haar, 1984), and the 1986 Northeastern Ohio earthquake (Wesson and Nicholson, 1986) and its aftershocks (Borcherdt, 1986; Borcherdt and Glassmoyer, 1987).

29. The trends shown in these data are consistent with the rock or stiff soil recordings of strong ground motion. They indicate a significant and reasonably consistent difference in high frequency spectral content between the representative rock motion in the WNA and ENA crust.

PART V: GENERATION OF SYNTHETIC TIME HISTORIES

Description of Technique

30. Synthetic time histories can be generated using a method based upon the capability of the BLWN model, with a simple ω-square constant-stress-parameter source, to reasonably predict a variety of measures of ground motion over a wide magnitude and distance range. Implied in this capability is that the general shape of the BLWN spectrum is an adequate representation, in many circumstances, of the physical process actually occurring in the earth. If it can be assumed that over the period range of engineering interest to critical facilities, 3 seconds to approximately 25 Hz or so, a critical facility cannot discriminate the Fourier amplitude spectrum between: 1) a simple point source approximation, instantaneous rupture over a circular fault zone and wave propagation in a uniform half-space; and 2) and a more rigorous representation of the earthquake source and wave propagation phenomena, then much of the difference may be contained in the phase spectrum. This is not an unreasonable assumption as the phase spectrum determines the distributing of energy in time and, as such, contains information regarding source, path, and site effects.

31. The technique of combining the phase spectrum from an observed strong motion record with the BLWN amplitude spectrum has been used to generate realistic time histories for a variety of source, path, and site conditions (Silva and Lee, 1987). In general, the results produced not only realistic acceleration time histories, but also integrations to velocity and displacement that appear indistinguishable from observed records as well. In order to produce synthetic records which have appropriate duration characteristics, the phase should be extracted from records of earthquakes with magnitudes within 1/2 unit of the design event (Silva and Lee, 1987). A suite of time histories may be quickly generated by combining different phases with the same

amplitude spectrum. Analyses performed with these time histories then impart the same spectral distribution of power into a system, but the distribution of levels of excitation in time will naturally differ for each input accelerogram.

32. As an example, local synthetic time histories are generated by combining the phase spectrum from a WNA strong motion record with the BLWN amplitude spectrum using both WNA and ENA source and propagation path operators (Table 1). While a phase spectrum from a WNA recording may not be appropriate for use in the context of an ENA tectonic environment, the assumption is that if any differences exist they may be significant only at high frequencies; beyond 20 Hz. At distances where the predominant motion is generated by phases (such as Lg) which do not propagate well in WNA, this assumption may not be valid. Additionally, due to differences in crustal structure between WNA and ENA coupled with the necessity to predict motion at large distances in ENA, circumstances exist where the simple BLWN model may not produce an adequate amplitude spectrum (Burger et al., 1987).

33. The BLWN model has also not been calibrated with data recorded from subduction zone earthquakes. At this time, no other recorded data are available to calibrate this technique for magnitudes greater than approximately M_w 7.5, or to verify the extrapolation of the recorded data into this magnitude and distance range.

34. Five-pole causal Butterworth filters are used with a high-pass corner at 8 seconds for both syntheses and low-pass corner at 23 Hz and 75 Hz for the WNA and ENA synthetics, respectively. The filtering was done to emulate some of the effects of processing.

Examples of Technique

35. Figures 6, 8, and 10 display synthetic and observed accelerograms for eastern North American rock sites for moment magnitudes (M_w) 6.0, 5.0, and 4.5, respectively. Accelerogram No. 1 (top time history) in each figure has been generated, as described in part V, by combining the phase spectrum from a recorded WNA accelerogram with the BLWN amplitude spectrum. Accelerograms No. 2 and No. 3 are observed ground motions at the appropriate magnitude and distance range recorded in the eastern United States. In each figure, the synthetic acceleration time history appears realistic with reasonable maximum acceleration, duration and distribution of energy in time. Also, the synthetic acceleration time history displays the typical non-stationarity contained in the observed ground motions. Figures 7, 9, and 11 are the 5% response spectral shapes for the synthetic and observed accelerograms shown in Figures 6, 8, and 10, respectively. Also, in each of these three figures the RVT estimate of the 5% response spectral shape is plotted (the dashed-dot curve). The RVT response spectral shape is smooth. The observed response spectral shapes, as well as, the response spectral shape computed from the syntnetic acceleration time history show characteristic peaks and valleys. In all three cases, the 5% response spectral shape generated by the method described above appears reasonable.

36. Figure 12 shows the acceleration, velocity, and displacement time histories using the WNA parameters. The peak accelerations and velocities were scaled by the respective peak values computed from the random process theory. The displacement time history is doubly integrated from the scaled acceleration time history. As can be observed from Figure 12, the time histories appear realistic with reasonable durations, distribution of energy in time, and display typical non-stationarity.

37. The results for ENA are shown in Figure 13. As expected, the acceleration time history displays more energy at higher frequencies than present in the WNA synthetic which is primarily due to the different value of kappa (Table 1). The WNA phase, taken from the same time history used for Figure 12 has been interpolated from a 50 Hz to a 200 Hz, Nyquist. Comparing the velocity and displacement time histories, we observe increasing similarity in amplitude with increasing predominant period between WNA and ENA synthetics. This effect is expected since the amplitude spectra at long periods between WNA and ENA differ only in Q effects and a slightly different corner frequency (due to stress-parameter and shear-wave velocity differences). These results are not inconsistent with indications of source similarity, in the frequency range of 0.3 - 1.0 Hz, between ENA and WNA earthquakes (Somerville et al., 1987).

38. Additionally, the 6 - 8 second period sinusoidal energy in the displacement time histories near 16 seconds is probably spurious. Moving the high-pass filter corner from 8 seconds to 5 seconds would largely eliminate this probable noise and leave the motion for periods shorter than 5 seconds largely unperturbed.

39. In order to compare the random process estimation of response spectral shapes to time domain spectral calculations, we have computed spectral shapes from the synthetic acceleration time histories. Figure 14 shows the response spectral shape computed from the WNA synthetic record plotted with the shape estimated by the random process (taken from Figure 8). Figure 15 shows the results for the ENA synthesis. In general, the random process model does a good job in estimating peak values of both acceleration and oscillator response. Apparently, the randomness of the phase spectrum is sufficient to produce a realistic oscillatory nature in the response spectra.

PART VI: GROUND MOTIONS FOR NEW MADRID EVENT

Summary of Model Parameters

40. The estimates of the source and path parameters used in the BLWN ground motion model are summarized below. It is important to emphasize that the estimated ground motion is on competent rock with a shear wave velocity estimated at 3.5 km/sec and a $Q(f) = 500\ (f)^{0.65}$. The maximum moment magnitude for a New Madrid earthquake is estimated to be 7.9 (Hanks and Kanamori, 1979) using the Nuttli (1983) estimate of 7.9×10^{27} dyne-cm for the seismic moment. The epicentral distance is 0 km and the hypocentral distance is 10 km consistent with the depths of microearthquakes betwen 5 and 15 km. The acceleration spectral density fall off is modeled by a kappa operator with $\kappa = 0.006$ sec.

41. The BLWN amplitude spectra estimated with the above parameters (see Table 1) is combined with the phase spectrum from an observed strong motion record using the technique demonstrated by Silva and Lee (1987). The two most important criteria in selecting the phase, so that the synthetic records will be appropriate, are that the seismic moments (magnitudes) of the earthquake and the design event and the source to site distances should be comparable. These criteria produce synthetic records with appropriate durations and timing of the major phase arrivals, so that the distribution of energy with time in the synthetic appears reasonable.

42. To satisfy these criteria, the accelerogram recorded at La Villita during the 19 September 1985 Michoacan, Mexico earthquake was selected. The Michoacan earthquake had a seismic moment estimated at 10.3×10^{27} dyne-cm, $M_s = 8.1$, $m_b = 7.0$, and a fault rupture area of approximately 170 km (length) by 50 km (width) (Anderson et al., 1986a, 1986b). These parameters compare favorably with the New Madrid parameters discussed in Part II of this report.

43. Secondly, the accelerogram at La Villita was situated directly above the aftershock zone and inferred rupture area of the mainshock. La Villita was located 43.7 km from the epicenter and 0.0 km from the outline of the aftershock zone of the 1985 Michoacan, Mexico earthquake. Peak horizontal ground acceleration are about 0.15g with bracketed durations of shaking in excess of 0.1 g of about 20 seconds. The phase of the La Villita accelerogram records the complex rupture process of the 1985 mainshock. There were two "sub-events," during the rupture process in which the release of seismic energy was more intense, separated by approximately 24 seconds. (Anderson, et al., 1986a, 1986b).

44. Also, the site conditions at La Villita are comparable to the site conditions used in the BLWN modeling. A compressional wave velocity of 5.6 km/sec has been measured from rock samples taken from the site at La Villita (Anderson et al., 1986b). Assuming a Poisson's ratio of 0.25, a shear wave velocity of 3.2 km/sec can be inferred. This value is near the selected value of 3.5 km/sec in the BLWN model. Thus, the phase from the La Villita accelerogram (N00°E component) is probably an appropriate description of the distribution of energy with time for a New Madrid event. A suite of appropriate time histories could be generated by using, for example, the other component of horizontal ground acceleration at La Villita, or the horizontal accelerograms recorded at Caleta de Campos and La Union.

45. While one may justifiably comment on the appropriateness of mixing the phase spectrum from a subduction zone event with the amplitude spectrum modeled to reflect an interplate event, the implicit assumption in this process is the inability to discriminate these types of events given only Fourier phase spectra.

46. Lastly, the recorded time history at La Villita with a Nyquist frequency of 50 Hz (100 samples/sec) is interpolated to a

Nyquist frequency of 100 Hz (200 sample/sec) before the phase spectrum is extracted for use in the BLWN ground motion model.

RVT Estimates of Peak Values

47. As discussed in section III, the BLWN ground motion model estimates a RMS value for the peak ground acceleration and velocity. From the RMS value, the peak ground motion value is estimated. For a M_w = 7.9 event at a hypocentral distance of 10 km, the RMS acceleration and velocity are 0.40 g and 39.2 cm/sec, respectively. The peak acceleration and velocity are 1.60 g and 124.2 cm/sec, respectively. These median values represent the BLWN point-source prediction for a maximum magnitude New Madrid event at a hard rock outcrop.

48. Interestingly, employing an increasing stress relation as proposed by Nuttli (1983) results in nearly identical ground motion values. This result occurs because the stress parameter in the increasing-stress model is 87 bars for an M_w = 7.9 which is close to the adopted value of 100 bars for ENA (Table 1). The corresponding corner periods for a moment of 7.9×10^{27} dyne-cm are 27 and 25 seconds respectively. Boore and Atkinson (1987) point out that both models, constant stress parameter and increasing stress parameter predict identical ground motion parameters at a moment magnitude of 8.1, very close to our assumed maximum new Madrid M_w of 7.9.

Acceleration, Velocity and Displacement Time Histories

49. Figures 16, 17 and 18 show the synthetic acceleration, velocity, and displacement time histories computed for a maximum magnitude (M_w=7.9) New Madrid event on competent rock. The BLWN Fourier amplitude spectrum has been combined with the phase spectrum from La Villita to produce the time histories. The acceleration and velocity

time histories have been scaled to the RVT predicted values of 1.60 g and 124.2 cm/sec, respectively. The unscaled peak particle velocity obtained by integrating the scaled acceleration record is 148.9 cm/sec. The displacement time history was produced by doubly integrating the scaled acceleration record and has a value of 102.9 cm. The five to ninety-five percent root-mean-square duration is 55.5 seconds (Dobry, Idriss, and Ng; 1978). For all three time histories, the time sample interval is 0.005 seconds with a corresponding Nyquist frequency of 100 Hz. The ground acceleration, velocity, and displacement time histories have been high-pass filtered with a five-pole Butterworth filter with a corner at 10 seconds. The ground acceleration time history is rich in high frequency components, consistent with an eastern United States propagation path length of 10 km. The peak acceleration occurs at approximately 43 seconds in the record. Both the ground velocity and displacement time histories have the peak motion associated with a pulse between 8 and 12 seconds into the record. Generally, the dominant period of the ground motion increases with time in the record.

50. All three time histories in Figures 16, 17, and 18 appear realistic with reasonable durations, peak values, distribution of energy in time and display typical non-stationarity.

Response Spectral Shape

51. Figure 19 shows the 5% damping response spectral shape (Sa/amax) for the BLWN ground motion model computed by RVT as well as the spectral shape computed from the synthetic time history. For both of these spectra, the Fourier amplitude spectral densities are identical. The time domain and the frequency domain estimates of Sa/amax are similar in spectral content.

Comparisons with Attenuation Results

52. Since there are no recordings of ground motions from large magnitude intraplate earthquakes at close distances to the source, the motions predicted for the maximum New Madrid earthquake by the WES-RASCAL model cannot be compared with empirical data. Comparisons with estimates based on published attenuation relationships are similarly limited because of the lack of data available for use in the regression analyses typically performed to develop the relationships. Nevertheless, in this section the motions predicted by the BLWN model will be compared with extrapolations of published relationships for ground motions in the central or eastern United States.

53. Campbell (1981) used recorded data from the western United States and accounted for observed differences in the absorption characteristics between the western and central United States to develop acceleration attenuation relationships for the central United States. Quadratic relationships with magnitude were used to fit absorption coefficients published by Nuttli for both regions. Attenuation relationships were developed for both epicentral and fault distance. The results are presented for magnitudes up to m_b = 6.5 and distances as close as 10 km (both fault and epicentral distances). For a magnitude m_b = 6.5 event and a distance of 10 km, the epicentral relationship results in an estimated peak acceleration of 0.86g which is over twice the value of 0.40 g estimated from the fault distance relationship. For m_b = 7.4 at a distance of 10 km the relationships show even greater differences in peak acceleration: 0.68g using fault distance and 3.36g using epicentral distance. The RVT estimate of 1.60g falls somewhat below the average of these two values.

54. Nuttli and Herrmann (1978) developed an attenuation relationship for the central United States based on correlations relating acceleration, site intensity, magnitude, and distance.

Extrapolations of the recommended relationship result in a peak acceleration of 3.13g in the epicentral region for a m_b 7.4 earthquake. Nuttli and Herrmann point out, however, that large accelerations result when the equation is extrapolated to the New Madrid earthquakes of 1811-1812, and that "there are no existing data which can be used to verify the extrapolations to such large magnitude earthquakes."

55. Nuttli and Herrmann (1984) used a semi-theoretical approach to develop relationships for peak acceleration, velocity, and displacement in the Mississippi Valley. The relationship uses a magnitude dependent depth term and a frequency dependent coefficient of anelastic attenuation. In this model the depth of the source increases with magnitude, thus the peak ground motions for large magnitude earthquakes tend to saturate at closer distances. For a m_b 7.4 earthquake, the minimum focal depth is calculated to be 44 km, and the peak acceleration, velocity, and displacement are 0.82g, 272 cm/sec, and 841 cm, respectively. According to their 1978 report, the source depth is at most 15 km for the central United States. The estimate of peak acceleration using WES-RASCAL methodology is over twice as large, primarily due to the shallower focal depth of 10 km. If a focal depth of 44 km were used in the WES-RASCAL analysis, lower peak accelerations than those from Nuttli and Herrmann's (1984) relationship would be estimated. Interestingly, the average of the extrapolations of the 1978 and 1984 relationships is near the value predicted by the WES-RASCAL analysis. It should be pointed out that the Nuttli and Herrmann attenuation relationships are probably most appropriate for a deep soil site.

56. Toro and McGuire (1987) and Boore and Atkinson (1987) used a BLWN approach to estimating peak acceleration and response spectral values of ground motions for sites founded upon rock in eastern North America. The BLWN model was used to estimate values through which an

equation was fit. Toro and McGuire used the m_{Lg} scale and Boore and Atkinson used the moment magnitude, M_w, scale. For a m_{Lg} 7.4, the Toro and McGuire relationship results in a peak acceleration of 1.56g at a distance of 10 km. For a M_w 7.9, the Boore and Atkinson relationship results in a peak acceleration of 1.98g at a distance of 10 km. Values of response spectral shape were also calculated for each set of relationships, as shown on Figure 20 with the estimated response spectral shape from WES-RASCAL. It must be emphasized that the relationships were not intended to be used at such extreme values of magnitude and distance, and these results can only be considered extrapolations of the published relationships. These two relationships give comparable results to the predictions from WES-RASCAL, which is not unexpected since all three are based on the BLWN method.

57. Krinitzsky, Chang, and Nuttli (Krinitzsky, Chang, and Nuttli; 1987) developed charts and curves relating magnitude and distance to peak acceleration, velocity, and duration for different site and source conditions. The curves for plate boundary earthquakes with focal depths less than or equal to 19 km give a mean horizontal acceleration of 1236 cm/sec^2 and a mean horizontal velocity of 94 cm/sec at a hard site for a magnitude 7.5 event. If extrapolated to a moment magnitude 7.9, the resulting values would be approximately 1.8g and 147 cm/sec. It must also be emphasized that these relationships were developed for plate boundaries, and are being used for an intraplate source. In addition, the magnitudes are being extrapolated beyond the original range.

58. All of these relationships and the results of the WES-RASCAL analyses are quite sensitive to variations in the input seismic moment (or magnitude) and distance. For relatively small variations in distance or magnitude, quite large differences in peak values can result. The assumptions of a point source of energy release used in the BLWN model clearly makes the method very sensitive to distance when estimates are made at distances much smaller than the dimensions of the

actual rupture. As described in Part II, the estimated rupture surface of the largest of the 1811-1812 earthquakes is 70 km long and 40 km wide. Energy is released non-uniformly over this entire surface, and not at a single point. As a result, the point source approximation does not predict saturation of ground motion values with increasing moment magnitude, and results in predictions for very large earthquakes that should be considered conservative.

PART VII: EFFECTS OF DEEP SOILS

59. In order to illustrate the effects of a deep soil profile upon the computed outcrop motion, time histories as well as response spectra are computed at the surface of a generic sand-like profile. The profile (Figure 21) is based upon a generic sand profile developed by the Electric Power Research Institute (Toro et al., 1987) as appropriate for deep sand-like sites in the central United States. The material density for the profile is taken as 2.1 g/cm^3. A small strain damping profile, in terms of the shear-wave quality factor Q_S, has been taken as $Q_S = 30\ V_S^{1.25}$ (km/sec) (Apsel et al., 1982). A lower bound of 16 for Q_S (3% damping ratio, $\eta \approx 50/Q_S$) was used (Joyner et al., 1981).

60. For levels of ground motion expected in the near-source region of a maximum magnitude New Madrid type event, traditional dynamic soil models would predict significant nonlinear soil response for saturated sands. Indeed, evidence of soil failure, such as, sand boils which occurred during the 1811-1812 New Madrid events indicates that nonlinear soil response should be accommodated in the computation of the motion expected at the surface of the profile.

Material Nonlinearities

61. It is well known from laboratory testing that soils exhibit pronounced nonlinear behavior under shear loading conditions. Shear modulus decreases with increasing strain with an accompanying increase in material damping (Drnevich et al., 1966; Seed and Idriss, 1970; Seed et al., 1984). If this observation is applicable to in-situ soil properties subject to earthquake loading, then site response calculations must accommodate these strain dependencies as material nonlinearities.

62. The strain dependence of soil moduli and material damping has been well documented in numerous laboratory studies for sands and clays (Drnevich et al., 1966, 1967; Seed and Idriss, 1970, 1984; Hardin and Drnevich, 1972; Silver and Seed, 1971). Various parametric relationships have been proposed to determine values of maximum shear modulus (at small strain levels) and variations of shear modulus and material damping with strain (Hardin and Drnevich, 1971; Martin, 1975). Nonlinear soil models which have been primarily developed from laboratory test results and utilized in dynamic analyses, include the Ramberg-Osgood model (Streeter et al., 1974; Faccioli et al., 1973; Idriss et al., 1978), an elasto-plastic model (Richart, 1975), Iwan-type model (Joyner and Chen, 1975; Dames & Moore and Science Applications, Inc., 1978: and Taylor Larkin, 1978), the hyperbolic model (Hardin and Drnevich, 1972), the endochronoic model (Day, 1975), and the Davidenkov model (Martin, 1975; Pyke, 1979).

63. Each of the nonlinear models mentioned has certain limitations and advantages in describing the response of soils to the type of loading produced by seismic disturbances. An effort has been made in some models to predict permanent deformations, while others have included pore pressure build-up and dissipation. Strain dependency of material properties from laboratory data is universally observed. It is reproducible and becomes significant for high levels of earthquake loading, i.e., strains > 10^{-2}%.

Implications for Site Response Calculations

64. Clearly if in-situ soil is behaving as laboratory-derived models suggest, nonlinear effects must be incorporated into site response analyses. In general, strain dependence of moduli and damping would result in a nonlinear wave equation with the full finite strain terms (Biot, 1965; Murnaghan, 1937). In this case, superposition is invalid, the wave equation does not separate into P, SV, and SH fields,

and Fourier analysis cannot be applied. The approach generally adopted is to assume infinitesimal displacements, utilize a linear wave equation, and confine the nonlinearity to the constitutive relation.

65. If a nonlinear constitutive relation is utilized, then velocities and damping become strain dependent. This can result in a wavefield and site response that depart significantly from linear one dimensional theory. For high levels of motion strain dependent wave velocities would generally result in a longer characteristic site period. Strain-dependent damping would generally reduce overall response at high strain levels. Depending upon site structure and input motion, these effects could be very large.

Conventional Computational Scheme

66. The computational scheme which has been most widely employed to evaluate one-dimensional site response assumes vertically propagating plane shear-waves. Departures of soil response from a linear constitutive relation are treated in an approximate manner through the use of the equivalent-linear approach.

67. The equivalent-linear approach, in its present form, was introduced by Seed and Idriss (1970). This scheme is a particular application of the general equivalent linear theory introduced by Iwan (1967). Basically, the approach is to approximate a second-order nonlinear equation, over a limited range of its variables, by a linear equation. Formally this is done in such a way that an average of the difference between the two systems is minimized. This was done in an ad hoc manner for ground response modeling by defining an effective strain which is assumed to exist for the duration of the excitation. This value is usually taken as 65% of the peak time-domain strain calculated at the midpoint of each layer, using a linear analysis. Moduli and

damping curves are then used to define new parameters for each layer. The linear response calculation is repeated, new effective strains evaluated, and iterations performed until the changes in parameters are below some tolerance level. Generally a few iterations are sufficient to achieve a strain-compatible linear solution.

68. This stepwise analysis procedure was formalized into a one-dimensional, vertically propagating shear-wave code termed SHAKE (Schnabel, Lysmer, and Seed; 1972). Subsequently, this code has become easily the most widely used analysis package for one-dimensional site response calculations.

69. The advantages of the equivalent-linear approach are that parameterization of complex nonlinear soil models is avoided and the mathematical simplicity of linear analysis is preserved. A truly nonlinear approach requires the specification of the shapes of hysteresis curves and their cyclic dependencies. In the equivalent-linear methodology the soil data are utilized directly and, because at each iteration the problem is linear and the material properties are frequency independent, the damping is rate independent and hysteresis loops close.

70. The most significant advantage of the equivalent-linear formulation is the preservation of the superposition principle. For linear systems, this principle permits spectral decomposition and frequency-domain solutions. One can then make use of the propagator matrix solution scheme (Haskell, 1960; Schnabel et al., 1972; Silva, 1976) for very efficient frequency domain solutions of the wave equation. The superposition principle then permits a spectral recomposition of the wavefields (sum over frequencies) through an inverse Fourier or Laplace transform. A non-subtle result of this is that the deconvolution process, that of propagating the control motion down rather than up, results in a unique solution. That is, for a given

motion at the surface, within an equivalent-linear framework there is only one base motion (solution). In reality of course, if the soils are behaving in a nonlinear fashion and have degraded, many different input motions at the base of the soil could have resulted in a similar surface response.

71. While the assumptions of vertically propagating shear-waves and equivalent-linear soil response certainly represent approximations to actual conditions, their combination has achieved demonstrated success in modeling observations of site effects (Schnabel et al., 1972; Silva et al., 1987).

Computational Scheme

72. The computational scheme employed to compute the site response uses the BLWN model to generate the power spectral density and spectral acceleration of the rock or control motion. This motion or power spectrum is then propagated through the one-dimensional soil profile using the plane-wave propagators of Silva (1976). In this formulation only SH waves are considered. Arbitrary angles of incidence may be specified but normal incidence is used throughout the present analyses. In order to treat possible material nonlinearities, the equivalent-linear formulation is employed. Random process theory is used to predict peak time domain values of shear-strain based upon the shear-strain power spectrum. In this sense the procedure is analogous to the program SHAKE except that peak shear strains in SHAKE are measured in the time domain. The purely frequency domain approach obviates a time domain control motion and, perhaps just as significant, eliminates the need for a suite of analyses based on different input motions. This arises because each time domain analysis may be viewed as one realization of a random process. In this case, several realizations of the random process must be sampled to have a statistically stable estimate of site response. The realizations are usually performed by

employing different control motions with approximately the same level of peak acceleration. In the case of the frequency domain approach the estimates of peak shear strain as well as oscillator response are, as a result of the random process theory, fundamentally probabilistic in nature. Stable estimates of site response can then be computed by forming the ratio of spectral acceleration predicted at the surface of a soil profile to the spectral acceleration predicted for the control motion. The procedure of generating the BLWN power spectrum, computing the equivalent-linear layered-soil response, and estimating peak time domain values has been incorporated into a code termed RASCALS.

Comparison of RASCALS with SHAKE

73. In order to demonstrate the appropriateness of site response computations using the frequency domain approach with random process estimates of ground motion as well as oscillator response, a comparison with results from SHAKE is presented. The soil profile used for the comparison is shown in Figure 22 and consists of a 120-foot thick stiff sand profile over rock. The modulus reduction and damping curves used in the analysis are shown in Figure 23. The variation of shear modulus with strain is taken as the upper range Seed-Idriss sand curve. The upper range was chosen as recent work on observations of site response (Silva et al., 1987) indicated that in-situ soil response to earthquake motions showed less shear-strain dependency of shear modulus than that predicted by the mid-range values. The variation in shear-wave damping with strain was modeled by using the mid-range as well as the lower-range Seed-Idriss sand curve (Figure 23). This was done to demonstrate the effects of the strain dependency of damping upon the computed motion. For the comparison with SHAKE, the mid-range damping curve was used.

74. Figure 24 shows the input and output time histories resulting from the SHAKE and RASCALS analyses. The time history on the top of the figure is a synthetic motion computed by RASCALS by combining the BLWN Fourier amplitude spectrum for a M_w = 6.5 ENA event at a hypocentral range of 8.5 km with the phase spectrum of an observed WNA event. In this case the f_{max} filter was used with an f_{max} of 40 Hz. The random process estimate of peak acceleration is approximately 1g. This motion is used as the rock outcrop or control motion input to SHAKE. The output from SHAKE is shown in Figure 24 (middle trace). The filtering effects of the soil column are easily seen with little effect on peak acceleration. The lower trace shows the results of the RASCALS analysis. In this case, the power spectrum of the input time history (top trace) is used as input. The output time history (bottom trace) is generated by combining the Fourier amplitude spectrum at the surface of the site with the phase spectrum from the outcrop motion (top trace). The two outputs, SHAKE (middle trace) and RASCALS (lower trace) are nearly indistinguishable. This indicates that the two approaches in estimating peak shear strains, time domain and random process theory, result in very nearly the same motion within the profiles. Of particular note, the peak acceleration at the surface of the profile predicted by the random process theory is 1.0g which is quite close to the 0.96g value resulting from the SHAKE analysis.

75. The 5% damped absolute acceleration response spectra of the control motion, SHAKE output, and the RASCALS analysis output are shown in Figure 25. The dotted line is the response spectrum computed in the time domain from the SHAKE output (middle trace in Figure 24). The smooth response spectra for the rock motion and for the surface of the soil (RASCALS output) are the random process estimates of oscillator response. As can be seen, the time domain results are rather oscillatory, due to the phase spectrum (Silva and Green, 1988), but generally follow the random process estimates. The figure clearly

demonstrates the necessity in averaging several time domain results, experimental or computational, in order to produce stable estimates of site response.

Results of Site Response Analysis

76. A suite of response analyses were performed in order to demonstrate the sensitivity of the motion computed at the surface of the profile to material damping. The suite of analyses consisted of linear, equivalent-linear with mid-range damping, equivalent-linear with low-range damping, and equivalent-linear using the modulus reduction curve (Seed-Idriss upper range) for damping as well as for modulus reduction. The latter analysis was performed by applying the modulus reduction curve to the initial Qs (damping) structure to approximately account for the effects of confining pressure upon material damping.

77. The acceleration time history computed at the surface of the soil provile resulting from the linear analysis is shown in Figure 26. The RVT estimate of the peak acceleration is about 2.06g which indicates a net amplification of high frequency energy for this shear-wave velocity and Qs gradient. The peak particle velocity is 156 cm/sec giving a v/a_p ratio of about 74 cm/sec/g. The computed time history is very similar in appearance to the outcrop motion retaining much of the high frequency energy input at the base of the soil column. The average Qs for the profile is approximately 20 which is a reasonable value based upon in-situ measurements at soil sites (Joyner et al., 1981; Johnson and Silva, 1981).

78. Figure 27 shows the computed surface motion using the frequency domain equivalent-linear technique with the low-range damping curve and the upper range modulus reduction curve. The motion is plotted to the same scale as that of the linear analysis and rather dramatically indicates the effects of nonlinear dynamic soil response.

The peak acceleration has been reduced to 0.78 g while the peak particle velocity has been only slightly reduced to 153 cm/sec. The v/a_p ratio is about 196 cm/sec/g which is close to values one would expect from strong motion at a deep site (Mohraz, 1976).

79. Results from the analysis using mid-range damping with upper range modulus reduction are shown in Figure 28. As expected, the peak acceleration has been further reduced, to 0.54 g, and the peak particle velocity is now 143 cm/sec. The v/a_p ratio is now increased to 265 cm/sec/g which seems rather high. The filtering effects of the increased damping are clearly visible in Figures 26 through 28 in going from the linear to the equivalent-linear analysis employing first lower- and then mid-range damping curves.

80. Figure 29 shows the results of the equivalent-linear analysis using the upper range modulus reduction curve for both shear-wave velocity as well as damping. In this analysis, the initial Qs structure or profile is assumed to obey the same strain dependency as the shear modulus. The peak acceleration is 0.88g and the peak particle velocity is now 162 cm/sec giving a V/a_p ratio of 184 cm/sec/g. These levels of motion are comparable to those resulting from the analysis using the lower range damping curve. They are somewhat higher reflecting lower levels of damping in the deeper part of the profile. This is a consequence of using an initial damping or Qs profile which reflects lower levels of damping (higher Qs) at low strains ($\leq 10^{-4}$%)) as depth increases.

81. The wide range in predicted peak acceleration values indicates the sensitivity of site response analyses for deep sites to assumed models of soil damping at high strain levels (Table 5). At the present time, no in-situ observations of shear-wave damping in soils are available to assess the reasonableness of our model assumptions. Limited laboratory data do indicate, however, that shear-wave damping is

influenced to some extent by confining pressure as well as being strain dependent. At this time, however, only results from laboratory tests, such as shown in Figure 23, are available to provide direct measures of shear-wave damping at shear strains higher than 10^{-2}%.

82. As a consequence of the uncertainty in the shear-wave damping at high strains, judgement must be relied upon to provide an estimate of the range in peak acceleration expected at deep soil sites located in the source region of a maximum magnitude New Madrid earthquake. The average shear strains for the site response analysis (except near the surface where shear strain approaches zero) is approximateley 0.15%. At this level of shear strain, it is unreasonable to expect soils to behave in a linear manner. The value of 2.06g (Table 5) resulting from the linear analysis may then be considered an unreasonably high value. Recent preliminary work by Woodward-Clyde Consultants has indicated that the mid-range damping curve may provide excessive damping if used throughout a deep soil profile. The value of 0.54g resulting from the analysis using the mid-range damping should then also receive a low weight in consideration of a likely range in levels of motion. Interestingly, the values of 0.78g and 0.88g resulting from the low range damping and Qs-reduction analyses respectively, compare favorably with the Nuttli and Herrmann (1984) value of 0.82g for a site directly above a m_b=7.4 event in the Mississippi Valley. Caution must be exercised in this comparison, however, as the Nutti and Herrmann curves also predict a peak particle velocity of 272 cm/sec, considerably greater than the values of 153 cm/sec and 162 cm/sec resulting from the mid-range damping and Qs reduction analyses.

83. Without further information to constrain the shear-wave damping curves at high strain values, it is not possible at this time to preclude peak accelerations approaching those predicted for the low-range damping. Based upon current knowledge then, the results using the

low-range damping, with a peak acceleration of 0.78g, represent a reasonable estimate of motions expected at the surface of a deep soil profile at very close distances to a New Madrid product type event.

84. Figure 30 shows the RVT absolute acceleration response spectra computed for all of the analyses as well as that of the outcrop motion. The effects of damping in terms of filtering the high frequencies are clearly visible. Also of interest is the shift in spectral amplification over the outcrop motion for the softer sites. The predicted effects of a deep generic profile upon ground motion due to a New Madrid type event at very close ranges is to deamplify frequencies higher than approximately 10 Hz and to possibly amplify frequencies less than 3 Hz compared to hard rock motions. It is important to emphasize that these specific remarks would likely not apply in detail to motion appropriate to a WNA tectonic environment. This is a consequence of the different spectral content, for the same level of peak acceleration, present in the WNA motion (Figure 3).

PART IX: SUMMARY AND CONCLUSIONS

85. Response spectral shapes computed from the BLWN ground motion model combined with random vibration theory have been demonstrated to give reasonably good agreement to shapes computed from observed WNA and ENA recordings on rock. Comparisons were made for a moment magnitude of approximately 6 1/2 at distances predominately within 50 km of the source. A site dependent kappa of 0.03 sec appeared reasonable for WNA motions recorded on soft-rock (sedimentary) at a variety of sites while a kappa of 0.006 sec was required at ENA sites.

86. The ground motions estimated using the BLWN model for a maximum level New Madrid event are large. For a moment magnitude of 7.9 and a depth of 10 kilometers, the peak values of the RVT estimates of ground motion at a hard rock site with a shear wave velocity of 3.5 km/sec are as follows:

Peak acceleration	1.60 g
Peak velocity	124 cm/sec
Maximum 5% response spectral acceleration	4.06 g at 33 Hz
Maximum 5% response spectral velocity	206 cm/sec

87. A synthetic time history was generated using the BLWN estimate of the Fourier amplitude spectrum and the Fourier phase spectrum extracted from a motion recorded in the near-source area of the 1985 Michoacan, Mexico earthquake. The peak values of the synthetic time history of ground motion are as follows:

Peak acceleration	1.60 g
Peak velocity	147 cm/sec
Peak displacement	103 cm

88. These results are extremely sensitive to relatively small variations in the magnitude and depth of the earthquake due to the assumption in the model of a point source. Extrapolations of published attenuation relationships beyond their range of applicability are similarly sensitive, which is not surprising since some of the relationships are also based on the BLWN model.

89. In order to assess the effects of a deep soil site upon the computed outcrop motion, response analyses were performed for a variety of assumptions regarding the strain dependency of the shear-wave damping. Results of the analyses do indicate that for reasonable assumptions regarding the shear-wave damping, peak accelerations at the surface of deep soil sites will be lower than those associated with corresponding hard outcrop motion. A reasonable estimate of peak acceleration expected at a deep soil site due to a New Madrid type earthquake is approximately 0.78g. This value resulted from an equivalent linear soil response analysis using Seed-Idriss sand curves. Specifically, the upper range modules reduction curve was used along with the lower-range damping curve.

90. The estimated peak values, response spectra, and time history of the motion appear to be internally consistent. That is the ratios of the response spectral acceleration values and the peak velocity to the peak acceleration are within the range of values expected. The amplitudes of the estimated values are high; some greater than the largest values recorded. Since no data exists for sites close to a large intraplate rupture, the accuracy of the estimated values is difficult to evaluate. Due to the known shortcoming of assuming a point source for the earthquake with the distance from the source less than the source dimensions, the estimates for the outcrop motion are probably conservative. The degree of conservatism cannot be evaluated without additional data from actual events.

REFERENCES

Anderson, J. G., 1986a, Implication of attenuation for studies of the earthquake source: in Das, S., Boatwright, J., and Scholz, C., eds., Earthquake Source Mechanics, Geophysical Monograph 37, American Geophysical Union, Washington, D.C., pp. 311-318.

Anderson, J. G., 1986b, Seismic strain rates in the central and eastern United States: Bulletin of the Seismological Society of America, Vol.76, No. 1, pp. 273-290, February.

Anderson, J. G., and Hough, S. E., 1984, A model for the shape of the Fourier amplitude spectrum of acceleration at high frequencies: Bulletin of the Seismological Society of America, Vol. 74, No. 5, pp. 1969-1993, October.

Anderson, J. G., Bodin, P., Brune, J. N., Prince, J., Singh, S. K., Quass, R., and Onate, M., 1986a, Strong ground motion from the Michoacan, Mexico, Earthquake: Science, Vol. 233, pp. 1043-1049, September 5.

Anderson, J. G., Brune, J. N., Prince, J., Mena, E., Bodin, P., Onate, M., Quass, R., and Singh, S. K., 1986b, Aspects of strong motion from the Michoacan, Mexico Earthquake of September 19, 1985: Proceedings 18th Joint Meeting on Wind and Seismic Effects, Washington, D.C., May 12-16.

Atkinson, G. M., 1984, Attenuation of strong ground motion in Canada: Bulletin of the Seismological Society of America, Vol. 74, No. 6, pp. 2629-2953, December.

Biot, M. A., 1965, Mechanics of Incremental Deformations. New York: John Wiley and Sons.

Boore, D. M., 1983, Stochastic simulation of high-frequency ground motions based on seismological models of the radiated spectra: Bulletin of the Seismological Society of America, Vol. 73, No. 6, Part A, pp. 1865-1984, December.

Boore, D. M., 1986a, Short-period P- and S-wave radiation from large earthquakes: implications for spectral scaling relations: Bulletin of the Seismological Society of America, Vol. 76, No. 1, pp. 43-64, February.

Boore, D. M., 1986b, The effect of finite bandwidth on seismic scaling relationships: in Das, S., Boatwright, J., and Scholz, C., eds., Earthquake Source Mechanics, Geophysical Monograph 37, American Geophysical Union, Washington, D.C., pp. 311-318.

Boore, D. M., and Atkinson, G. M., 1987, Prediction of ground motion and spectral response parameters at hard-rock sites in eastern North America: Bulletin of the Seismological Society of America, Vol. 77, No. 2, pp. 440-467, April.

Boore, D. M., and Joyner, W. B., 1984, A note on the use of random vibration theory to predict peak amplitudes of transient signals: Bulletin of the Seismological Society of America, Vol. 74, No. 5, pp. 2035-2039, October.

Borcherdt, R. D., 1986, Preliminary report on aftershock sequence for earthquake of January 31, 1986 near Painesville, Ohio: U.S. Geological Survey, Open-File Report 86-181.

Borcherdt, R. D., and Glassmoyer, G., 1987, On the aftershock sequence for the earthquake of January 31, 1986 in northeastern Ohio; effects of band width and local geology on observed high-frequency ground motion: Workshop on Earthquake Ground Motion Estimation in Eastern North America, Electric Power Research Institute, March 31 - April 2.

Brune, J. N., 1970, Tectonic stress and the spectra of seismic shear waves from earthquakes: Journal of Geophysical Research, Vol. 75, pp. 4997-5009.

Brune, J. N., 1971, Correction: Journal of Geophysical Research, Vol. 76, pp. 5002.

Burger, R. W., Somerville, P. G., Barker, J. S., Herrmann, R. B., and Helmberger, D. V., 1987, The effect of crustal structure on strong ground motion attenuation relations in eastern North America: Bulletin of the Seismological Society of America, Vol. 77, No. 2, pp. 420-439, April.

Campbell, K. W., 1981, A ground motion model for the central United States based on near-source acceleration data: in Beavers, J. E., ed., Proceedings, Conference on Earthquakes and Earthquake Engineering - Eastern United States, Knoxville, Tennessee, September 14-16, Ann Arbor Science Publishers, Vol. 1, pp. 213-222.

Chang, C.-Y., Power, M.S., Idriss, I.M., Somerville, P.G., Silva, W., Chen., P.C., 1986, Engineering Characterization of Ground Motion. Task II: Observational Data on Spatial Variations of Earthquake Ground Motion. Prepared for U.S. Nuclear Regulatory Commission, NUREG/CR- 3805, vol. 3.

Cranswick, E., Wetmiller, R., and Boatwright, J., 1985, High-frequency observations and source parameters of microearthquakes recorded at hard-rock sites: Bulletin of the Seismological Society of America, Vol. 75, No. 6, pp. 1535-1567, December.

Dames & Moore and Science Application, Inc., 1978, Study of Non-Linear Effects on One-Dimensional Earthquake Response. Electric Power Research Institute NP-865 Projects 615-1, -2, Final Report, August.

Day, S. M., 1979, Three-Dimensional Finite Differences Simulation of Fault Dynamics. Systems, Science and Software Final Report sponsored by the National Aeronautics and Space Administration. SSS-R-80-4295.

Dobry, R., Idriss, I. M., and Ng, E., 1978, Duration characteristics of horizontal components of strong-motion earthquake records: Bulletin of the Seismological Society of America, Vol. 68, No. 5, pp. 1487-1520, October.

Drnevich, V. P., Hall, J. R., Jr. and Richart, F. E., Jr., 1966, Large Amplitude Vibration Effects on the Shear Modulus of Sand. University of Michigan Report to Waterways Experiment Station, Corps of Engineers, U.S. Army, Contract DA-22-079-eng-340, October.

Drnevich, V. P., Hall, J. R., Jr. and Richart, F. E., Jr., 1967, Effects of Amplitude of Vibration on the Shear Modulus of Sand. in Proceedings of the International Symposium on Wave Propagation and Dynamical Properites of Earth Materials, University of New Mexico, Albuquerque, New Mexico.

Faccioli, E.E., Santayo, V. and Leone, J.L., 1973. Microzonation Criteria and Seismic Response Studies for the City of Managua. in Proceedings Earthquake Engineering Research District Conference, Managua, Managua, Nicaragua, Earthquake of December 23, 1972 I, pp. 271-291.

Grant, W.P. and Brown, F.R., Jr., 1981, Dynamic Behavior of Soils and Field and Laboratory Tests. in International Conferences on Geotechnical Engineering, University of Missouri.

Haar, L. C., Fletcher, J. B., and Mueller, C. S., 1984, The 1982 Enola, Arkansas swarm and scaling of ground motion in the eastern United States: Bulletin of the Seismological Society of America, Vol. 74, No.6, pp. 2463-2482, December.

Hanks, T. C., 1982, fmax: Bulletin of the Seismological Society of America, Vol. 72, No. 6, pp. 1867-1879, December.

Hanks, T. C., and Kanamori, H., 1979, A moment magnitude scale: Journal of Geophysical Research, Vol. 84, pp. 2981-2987.

Hanks, T. C., 1979, b values and $\omega^{-\gamma}$ seismic source models: implications for tectonic stress variations along active crustal fault zones and the estimation of high-frequency strong ground motion, Journal of Geophysical Research, Vol. 84, pp. 2235-2242.

Hanks, T. C., and McGuire, R. K., 1981, The character of high-frequency strong ground motion: Bulletin of the Seismological Society of America, Vol. 71, No. 6, pp. 2071-2095, December.

Hardin, B. O., and Drnevich, V.P., 1972, Shear modulus and damping in soils: design equations and curves. Proceedings American Society Civil Engineering, Journal of the Soil Mechanics and Foundations Division 98, vol. 98, pp. 667-692.

Haskell, N.A., 1960, Crustal Reflection of Plane SH Waves. Journal of Geophysical Research, vol. 65, pp. 4147-4150.

Herrmann, R. B., and Canas, J. A., 1978, Focal mechanism studies in the New Madrid seismic zone: Bulletin of the Seismological Society of America, Vol. 68, No. 4, pp. 1095-1102, August.

Herrmann, R. B., Cheng, S., and Nuttli, O. W., 1978, Archeoseismology applied to the New Madrid earthquakes of 1811-1812: Bulletin of the Seismological Society of America, Vol. 68, No. 6, pp. 1751-1759, December.

Idriss, I. M., Dobry, R. and Singh, R. D., 1978, Non-linear behavior of soft clays during cyclic loading, Journal of the Geotechnical Engineering Division, American Society of Civil Engineers, Vol. 104, No. GT12, December, pp. 1427-1447.

Iwan, W. D., 1967, On a Class of Models for the Yielding Behavior of Continuous and Composite Systems. Journal of Applied Mechanics vol. 34, pp. 612-617.

Johnson, L.R. and W. Silva., 1981, The Effects of Unconsolidated Sediments upon the Ground Motion during Local Earthquakes. Bulletin of the Seismological Society of America, vol. 71, pp. 127-142.

Joyner, W.B. and Chen., A.T.F., 1975, Calculation of Nonlinear Ground Response in Earthquakes. Bulletin of the Seismological Society of America, vol 65, pp. 1315-1336.

Joyner, W.B., Warrick, R.E. and Oliver, A.A., 1976. Analysis of Seismograms from a Downhole Array in Sediments near San Francisco Bay. Bulletin of the Seismological Society of America, vol. 66, 1976, pp. 937-958.

Krinitzsky, E. L. and Chang, F. K., 1987, Parameters for Specifying Magnitude-Related Earthquake Ground Motions: State-of-the-Art for Assessing Earthquake Hazards in the United States, Report 26, U.S. Army Corps of Engineers Waterways Experiment Station, Vicksburg, Mississippi, Miscellaneous Paper S-73-1, 58. September.

Luco, J. E., 1985, On strong ground motion estimates based on models of the radiated spectrum: Bulletin of the Seismological Society of America, Vol. 75, No. 3, pp. 641-650, June.

Martin, P. P., Non-Linear Methods for Dynamic Analysis of Ground Response. Ph.D. Thesis, University of California, Berkeley, California, June 1975.

McGuire, R. K., and Hanks, T. C., 1980, RMS accelerations and spectral amplitudes of strong ground motion during the San Fernando, California, earthquake: Bulletin of the Seismological Society of America, Vol. 70,No. 5, pp. 1907-1920, October.

McGuire, R. K., Becker, A. M., and Donovan, N. C., 1984, Spectral estimates of seismic shear waves: Bulletin of the Seismological Society of America, Vol. 74, No. 4, pp. 1427-1440, August.

Mento, D. J., Ervin, C. P., and McGinnis, L. D., 1986, Periodic energy release in the New Madrid seismic zone: Bulletin of the Seismological Society of America, Vol. 76, No. 4, pp. 1001-1009, August.

Mohraz, B. J. A study of earthquake response spectra for different geologic conditions. Bulletin of the Seismological Society of America, vol. 66, no. 3, 1976, pp. 915-935.

Murnaghan, F. D., 1937. Finite Deformations of an Elastic Solid. American Journal of Mathematics, vol. 59, 1937, p. 235.

Murphy, J.R. and Laboud, J.A., 1969, Analysis of seismic peak amplitudes from underground nuclear detonations. Bulletin of the Seismological Society of America, vol. 59, pp. 2325-2342.

Nuttli, O. W., 1973a, Seismic wave attenuation and magnitude relations for eastern North America: Journal of Geophysical Research, Vol. 78, No. 5, pp. 876-885, February.

Nuttli, O. W., 1973b, The Mississippi Valley earthquakes of 1811 and 1812: intensities, ground motion, and magnitudes: Bulletin of the Seismological Society of America, Vol. 63, No. 1, pp. 227-248, February.

Nuttli, O. W., 1981, Similarities and differences between western and eastern United States earthquakes, and their consequences for earthquake engineering: in Beavers, J. E., ed., Proceedings, Conference on Earthquakes and Earthquake Engineering - Eastern United States, Knoxville, Tennessee, September 14-16, Ann Arbor Science Publishers.

Nuttli, O. W., 1983, Average seismic source parameter relations for mid-plate earthquakes: Bulletin of the Seismological Society of America, Vol. 73, No. 2, pp. 519-535, April.

Nuttli, O. W., 1986, Yield estimates of Nevada test site explosions obtained from seismic Lg wave: Journal of Geophysical Research, Vol. 91, pp. 2137-2151.

Nuttli, O. W., and Herrmann, R. B., 1978, Credible earthquakes for the central United States: State-of-the-Art for Assessing Earthquake Hazards in the United States, Report 12, U.S. Army Engineer Waterways Experiment Station, Vicksburg, Mississippi, Miscellaneous Paper S-73-1, 103 p., December.

Nuttli, O. W., and Herrmann, R. B., 1984, Ground motion of Mississippi Valley earthquakes: Journal of Technical Topics in Civil Engineering, America Society of Civil Engineers, Vol. 110, No. 1, pp. 54-69, May.

Papageorgiou, A. S., and Aki, K., 1983, A specific barrier model for the quantitative description of inhomogeneous faulting and the prediction of strong ground motion, Part II, Applications of the model: Bulletin of the Seismological Society of America, Vol. 73, No. 4, pp. 953-978, August.

Pyke, R., 1979, Nonlinear Soil Models for Irregular Cyclic Loadings. Journal of the Geotechnical Engineering Division, American Society of Civil Engineers, vol. 105, June p. 715.

Richart, F.E., 1975, Some Effects of Dynamic Soil Properties on Soil-Structure Interaction. Journal of the Geotechnical Engineering Divison, American Society of Civil Engineers, vol. 101, p. 1197.

Rogers, A.M. and Hays, W.W., 1978, Preliminary evaluation of site transfer functions developed from earhtquakes and nuclear explosions. Proceedings of the 2nd International Conference on Microzonation for Safer Construction-Research and Application, pp. 753-764.

Rogers, A.M. Tinsley, J.C., Hays, W.W. and King, K.W., 1979, Evaluations of the Relation Between Near-Surface Geological Units and Ground Response in the Vicinity of Long Beach, California. Bulletin of the Seismological Society of America, vol. 69, pp. 1603-1622.

Schnabel, P. B., Lysmer, J. and Seed, H. B., 1972. SHAKE - A Computer Program for Earthquake Analysis of Horizontally Layered Sites. Report No. EERC 72-12, Earthquake Engineering Research Center, University of California, Berkeley, California, December.

Seed, H. B., and Idriss, I. M. 1970a. Analysis of ground motions at Union Bay, Seattle, during earthquakes and distance nuclear blasts. Bulletin of the Seismological Society of America, vol. 60, no. 1, February, p. 125-136.

Seed, H. B., and Idriss, I. M., 1970b. Soil Moduli and Damping Factors for Dynamic Response Analysis. Report No. EERC 70-10, Earthquake Engineering Research Center, University of California, Berkeley, California, December.

Seed, H. B., and Idriss, I. M., 1984. Moduli and Damping Factors for Dynamic analyses of Cohesionless Soils. Report No. EERC-84/14, Earthquake Engineering Research Center, University of California, Berkeley, California, September.

Seed, H. B., Wong, R. T., Idriss, I. M., and Tokimatsu, K., 1984. Moduli and Damping Factors for Dynamic Analyses of Cohesionless Soils. Report No. EERC-84/14, Earthquake Engineering Research Center, University of California, Berkeley, California, September.

Shima, E. 1962, Modification sof seismic waves in superficial soil layers as verified by comparative observations on and beneath the surface. Bulletin Earthquake Research Institute, Tokyo University, vol. 40, pp. 187-259.

Silva, W. J., and Green, R. K., 1988, Magnitude and distance scaling of response spectral shapes for rock sites with applications to North American tectonic environments: paper submitted for publication to Earthquake Spectra, Earthquake Engineering Research Institute.

Silva, W. J., and Lee, K., 1987, WES RASCAL code for synthesizing earthquake ground motions: State-of-the-Art for Assessing Earthquake Hazards in the United States, Report 24, U.S. Army Corps of Engineers Waterways Experiment Station, Vicksburg, Mississippi, Miscellaneous Paper S-73-1, 120p., May.

Silva, W., J., T. Turcotte, and Y. Moriwaki, 1987, Soil response to earthquake ground motion. Electric Power Research Institute, Report NP-5747.

Silva, W. J., Body waves in a layered anelastic solid. Bulletin of the Seismological Society of America, vol. 66, 1976, pp. 1539-1554.

Silver, M. L. and Seed, H. B., 1971. Deformation Characteristics of Sands Under Cyclic Loading. Journal of the Soil Mechanics and Foundations Division, American Society of Civil Engineers. vol. 97, SM9, p. 1171.

Sommerville, P. G., McLaren, J. P., LeFevre, L. V., Burger, R. W., and Helmberger, D. V., 1987, Comparison of source scaling relations of eastern and western North American earthquakes: Bulletin of the Seismological Society of America, Vol. 77, No. 2, pp. 322-346, April.

Stauder, W., Kramer, M., Fischer, G., Schaefer, S., and Morrissey, S.T., 1976, Seismic characteristics of southeast Missouri as indicated by a regional telemetered microearthquake array: Bulletin of the Seismological Society of America, Vol. 66, No. 6, pp. 1953-1964, December.

Street, R., 1980, A compilation of accounts describing the Mississippi Valley earthquakes of 1811-1812: Part I: Department of Geology, University of Kentucky, Lexington.

Streeter, V.L., Wylie, E.B. and Richart, F.E., Jr., 1974. Soil Motion Computations by Characteristics Method. Journal of the Geotechnica Engineering Division, Proceedings, Amercian Society of Civil Engineers, Vol. 100, No. GT3, 1974, pp. 247-263.

Taylor, P.W. and Larkin, T.J., 1978, Seismic Site Response of Nonlinear Soil Media. Journal of the Geotechnical Engineering Division, American Society of Civil Engineers, vol 104, no. GT3, March.

Tokimatsu, K. and S. Midorikawa, 1981, Nonlinear Soil Properties Estimated from Strong Motion Accelerograms. International Conferences on Recent Advances in Geotechnical Earthquake Engineering and Soil Dynamics. Rolla, Missouri.

Toro, G. R., 1985, Stochastic model estimates of strong ground motion: in McGuire, R. K., ed., Seismic Hazard Methodology for Nuclear Facilities in the Eastern United States, Appendix B, Electric Power Research Institute, Project P101-29, April.

Toro, G. R. and R. K. McGuire, 1987, An investigation into earthquake ground motion characteristics in eastern North America. Bulletin of the Seismological Society of America, vol. 77, no. 2, April, pp. 468-489.

Toro, G. R., McGuire, R. K., and Silva, W. J., 1988, Engineering Estimates of Earthquake Ground Motion for Eastern North America, Electric Power Research Institute, Project RP2556-16, May.

Wesson, R. L., and Nicholson, C., 1986, Studies of the January 31, 1986 northeastern Ohio earthquake: Report to the U.S. Nuclear Regulatory Commission, U.S. Geological Survey, Open-File Report 86-331, 131 p., Reston, Virginia.

Wiechert, D. H., Wetmiller, R. J., Horner, R. B., Munro, P. S., and Mork, P. N., 1986, Strong motion records from the 23 December 1985, Ms 6.9 Nahanni, NWT, and some associated earthquakes: Geological Survey of Canada, Open File Report 1330.

Woods, R.D., 1968, Screening of Surface Waves in Soils. Journal of the Soil Mechanics and Foundations Division, Proceedings, American Society of Civil Engineers vol. 94. no. SM4, pp. 951-979.

TABLE 1

Earthquake Source and Wave Propagation Parameters

Parameters	Western North America (WNA)	Eastern North America (ENA)
ρ (g/cm^3)	2.7	2.5
β (km/sec)	3.2	3.5
kappa (sec)	0.03	0.006
Q(f)*	$150(f)^{0.6}$	$500\ (f)^{0.65}$
$\Delta\sigma$ (bars)	50	100
M_o (dyne-cm)	$\log M_o = 1.5\ M_w + 16.1$	$\log M_o = 1.5\ M_w + 16.1$
Amplification Factors	See Table 2	1.0
Geometrical Attenuation	R^{-1}	R^{-1}
Source Duration	f_c^{-1}	f_c^{-1}
f_c	$\beta^3\Delta\sigma/8.44\ M_o$	$\beta^3\Delta\sigma/8.44\ M_o$

* WNA from Nuttli (1986); ENA from Toro (1985)

TABLE 2

Near surface amplification factors (from Boore, 1986)

log frequency	$\log \left(\frac{\beta_o \rho_o}{\beta_R \rho_R}\right)^{\frac{1}{2}*}$
-1.0	0.01
-0.5	0.04
0.0	0.13
0.5	0.34
1.0	0.37

* ρ_o and ρ_R are assumed to be equal

o,R refers to average crustal properties and near-receiver properties, respectively.

TABLE 3

Earthquakes and Stations Used for ENA M_w = 6.5 Comparison

Earthquake	Date	Magnitude	Source Depth (km)	Epicentral Distance (km)	Station	Average Horizontal Peak Accleration (g)
Nahanni	851223	6.4 (m_b)	18	8	Site #1	1.18
			18	9	Site #2	0.47
			18	20	Site #3	0.19

TABLE 4

Earthquakes and Sites Used for WNA M_w = 6.5 Comparison

Earthquake	Date	Magnitude	Source Depth (km)	Epicentral Distance (km)	Station	No.	Average Horizontal Peak Acceleration (g)
San Fernando	710209	6.4 (M_L)	8.4	8.7	Pacioma	279	1.123
				36.1	Seis. Lab.	266	0.141
				27.3	Lake Hughes 4	126	0.159
				26.3	Lake Hughes 9	127	0.117
				23.0	Lake Hughes 12	128	0.318
				33.8	Griffith Park	141	0.176
				32.6	Fairmont	121	0.082
				43.2	Santa Anita	104	0.155
				70.4	Tehachapi	1027	0.036
Imperial Valley	791015	6.6 (M_L)	10.0	30	Superstition Mountain	286	0.165

TABLE 5

Results of Site Response Analyses

Analyses	Ap(g)	V(cm/sec)	V/Ap (cm/sec/g)
Outcrop	1.60	124	78
Linear	2.06	156	67
*Low-Range Damping	0.78	153	196
*Mid-Range Damping	0.54	143	265
*Qs Reduction **	0.88	162	184

* Equivalent-linear analyses using Seed-Idriss upper range modulus reduction curve for sand (Figure 23)

** Uses Seed-Idriss modulus reduction curve (Figure 23) to model strain dependency of initial (low-strain) Qs (damping) profile

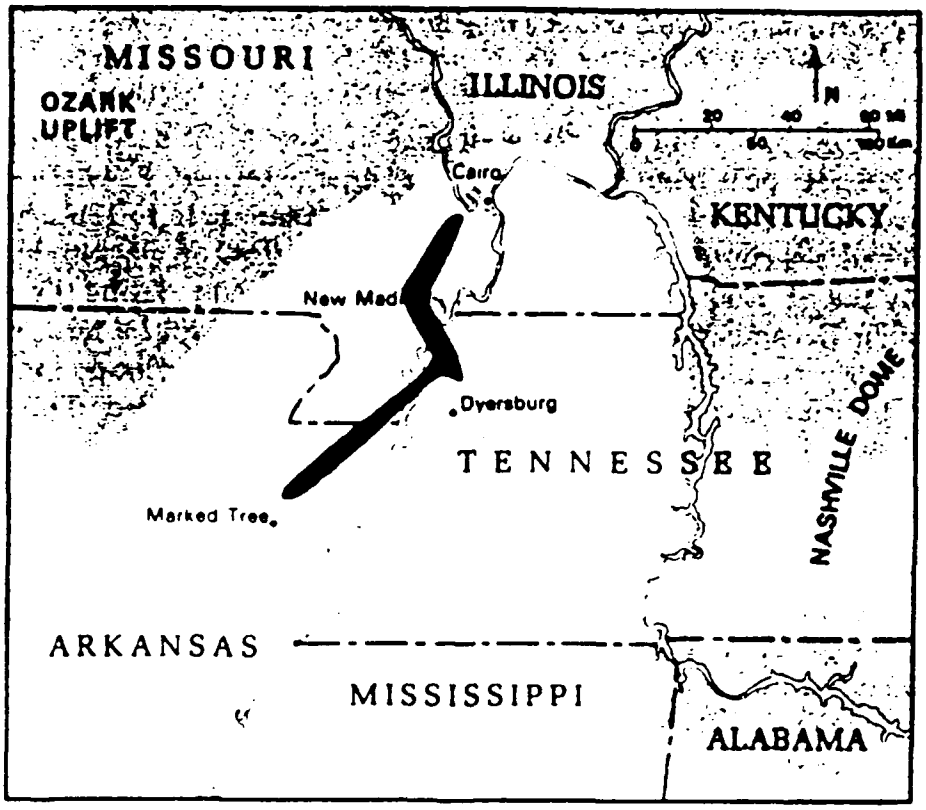

Figure 1 - Location of New Madrid seismic zone primary fault segments. Figure taken from Mento, et al., 1986.

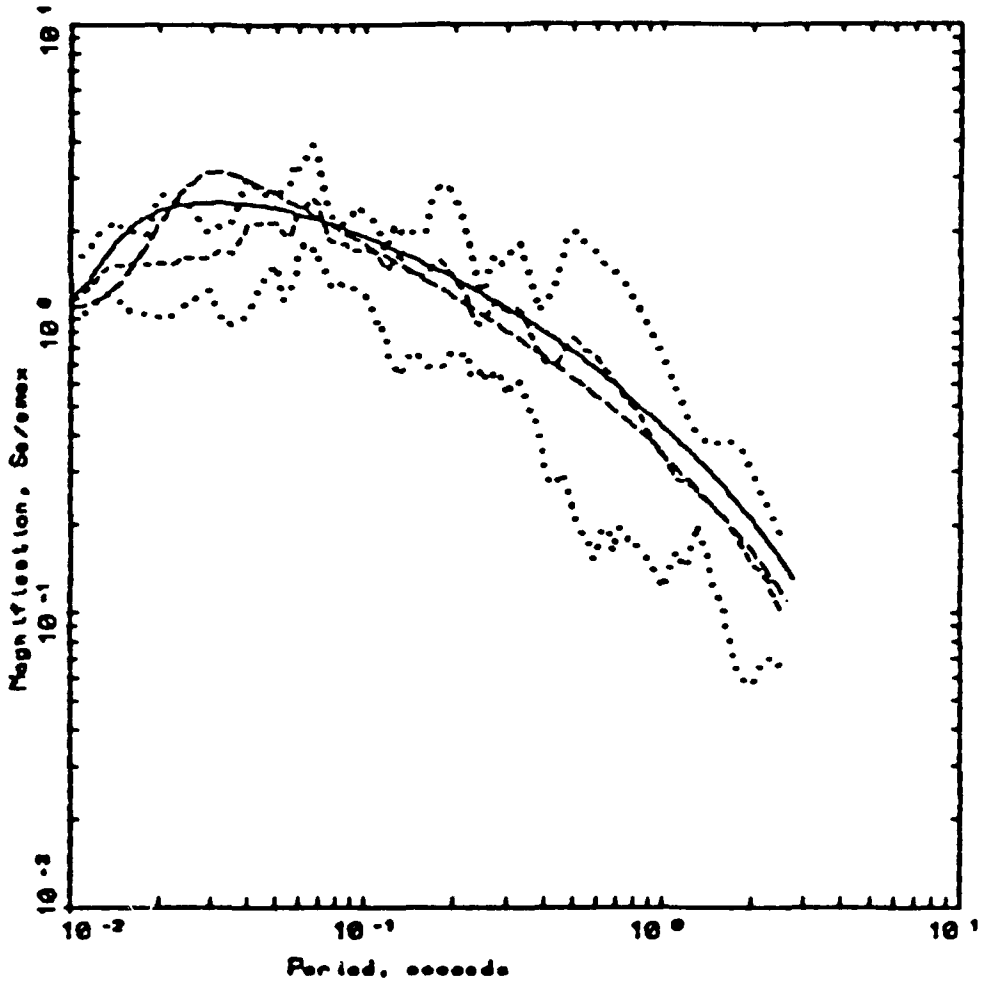

Figure 2 - Comparison of predicted 5% response spectral shape (solid lines) for a moment magnitude (M_w) 6.4 earthquake at a distance of 25 km using ENA parameters (Table 1) and either f_{max} = 40 Hz or kappa = 0.006 with the average shape (dashed line) from recorded data (Table 3). The dotted lines represent extremes of the shapes computed from the recorded data.

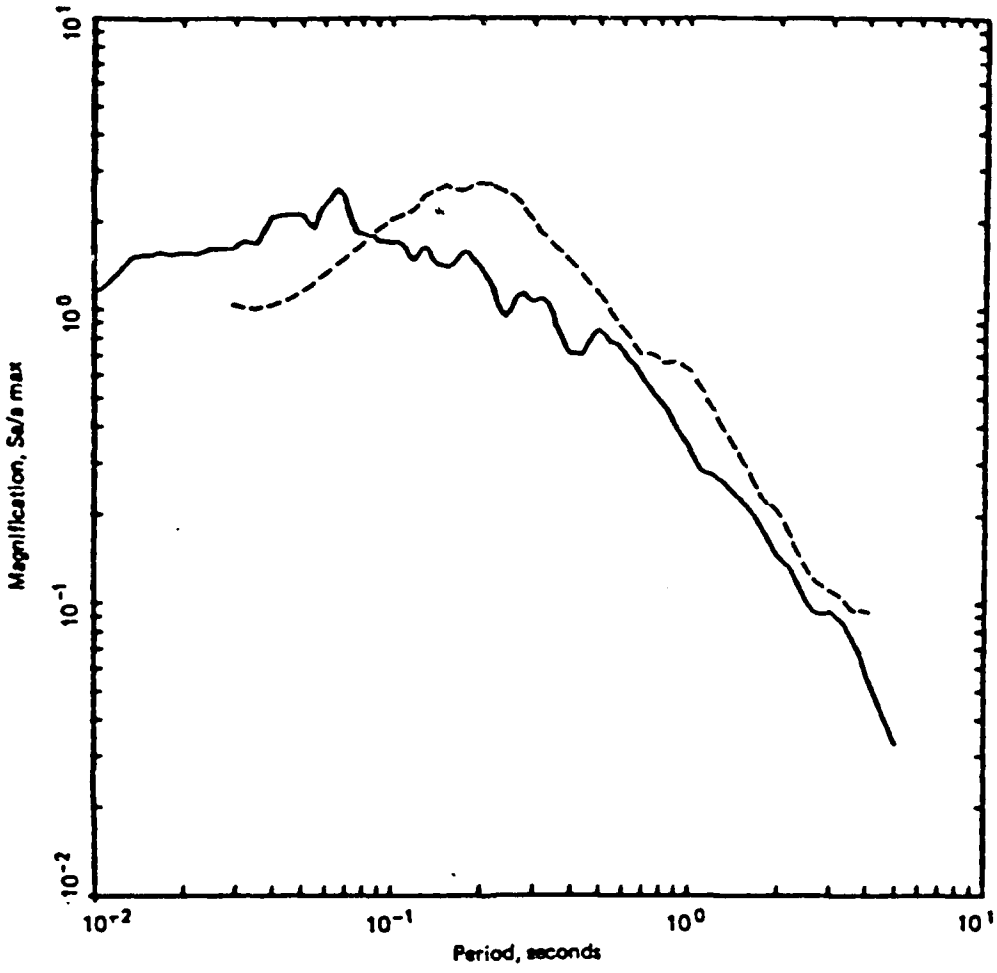

LEGEND

——— 5%, Nahanni mb = 6.4 rock readings

– – – – 5%, San Fernando ML = 6.4, Imperial Valley 79 ML = 6.6 rock recordings

Figure 3 - Comparison of average 5% response spectral shapes (Sa/a_{max}) computed from strong motion data recorded at rock sites in ENA (solid line) and WNA (dashed line). ENA average shape is from recordings of the m_b = 6.4 Nahanni aftershock. The WNA average shape is from recordings of the San Fernando M_L = 6.4 and Imperial Valley M_L = 6.6 events.

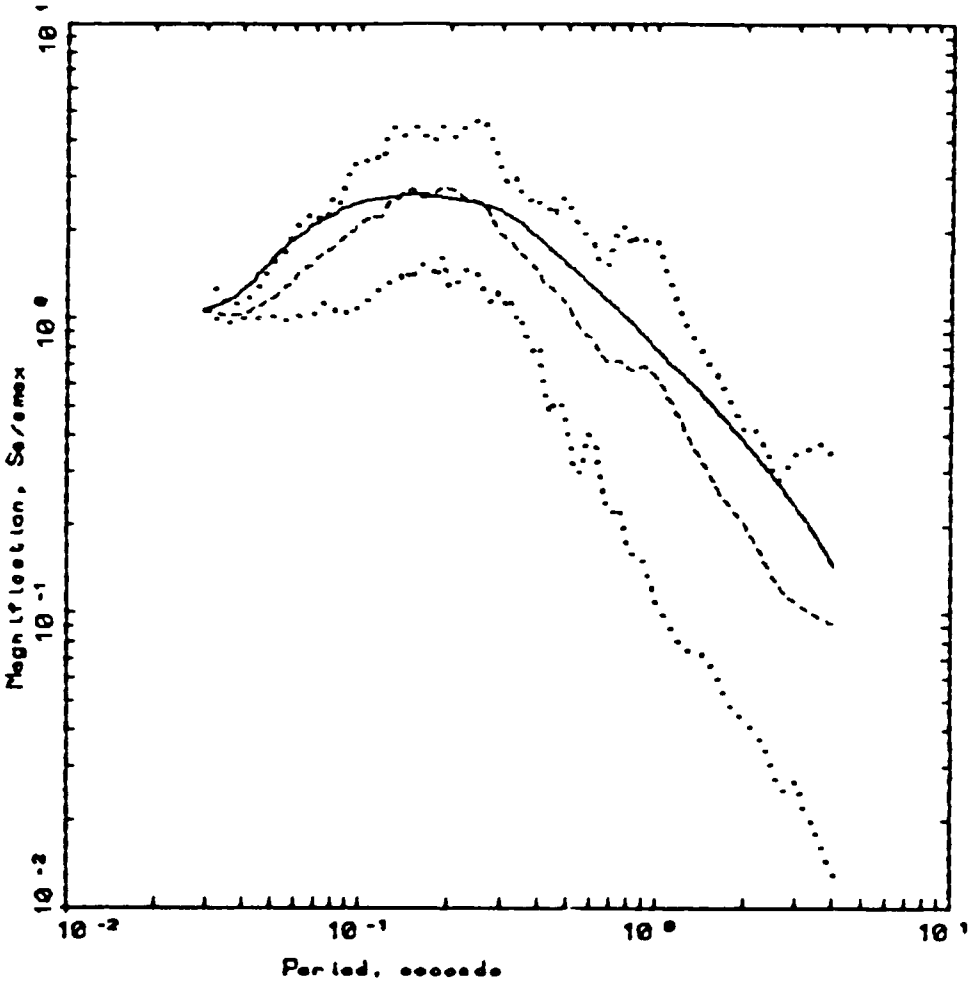

Figure 4 - Comparison of predicted 5% response spectral shape (solid line) for a moment magnitude (M_W) 6.5 earthquake at a distance of 25 km using WNA parameters (Table 1) with average shape computed from recorded data (Table 4, dashed line). The dotted lines represent the extremes of the shapes computed from the recorded data.

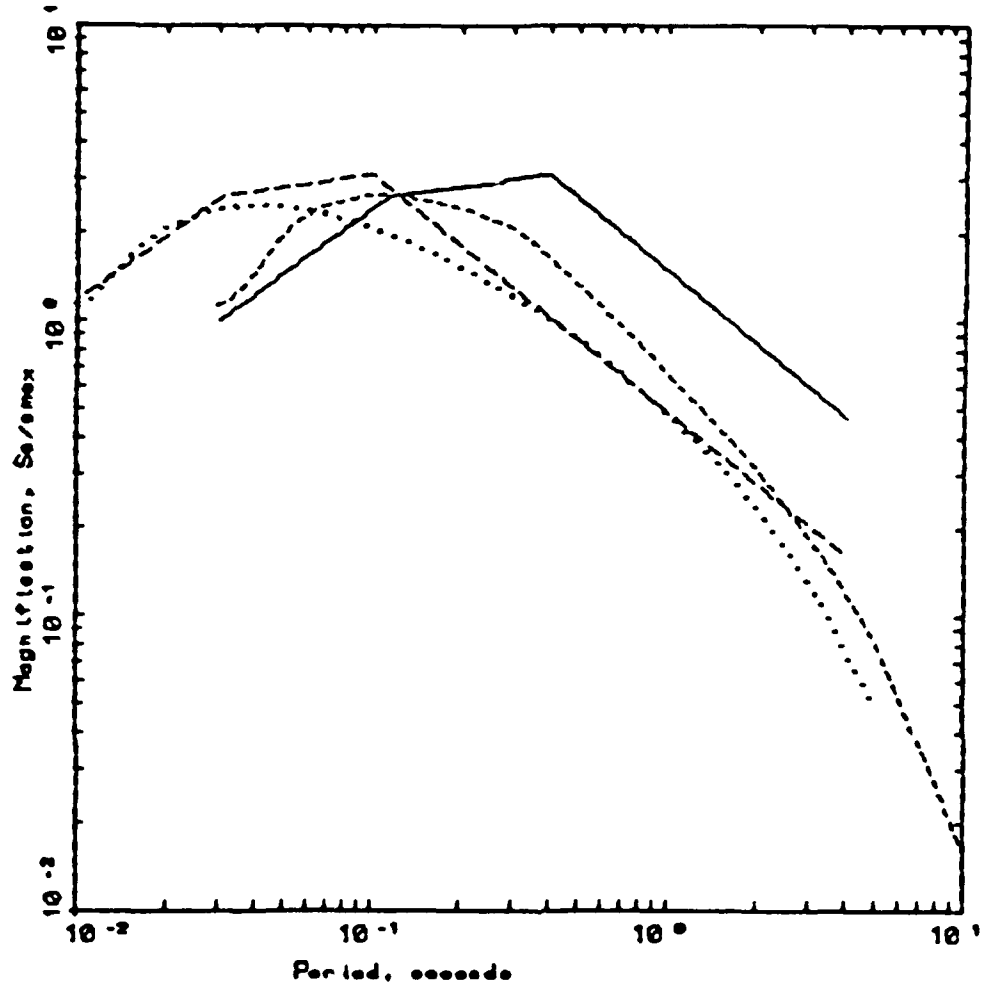

Figure 5: Comparison of predicted 5% response spectral shapes for ENA (dotted line) and WNA (dashed line) from Table 1 to the Nuclear Regulatory Commission's response spectral shape (Regulatory Guide 1.60) (solid line). The long-dashed line is the Reg. 1.60 shape with control points A, B, and C moved to 125, 33, and 10 H_z respectively.

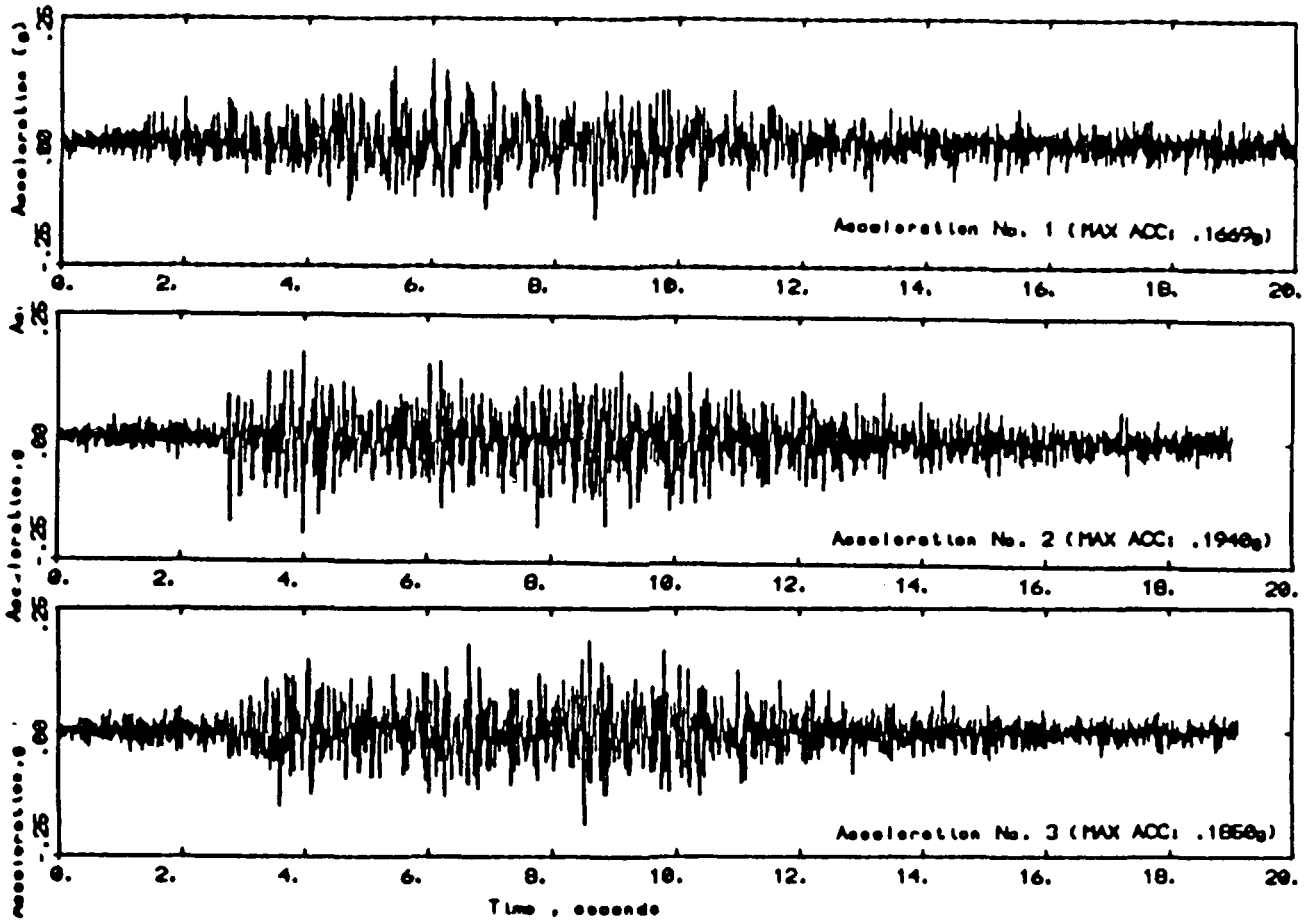

Figure 6 - Comparison of a synthetic accelerogram (Acceleration No. 1) generated as described in Part V to two examples of recorded ground accelerations (Accelerations No. 2 and No. 3) at a distance of 25 km for M_W = 6.0 using ENA parameters (Table 1).

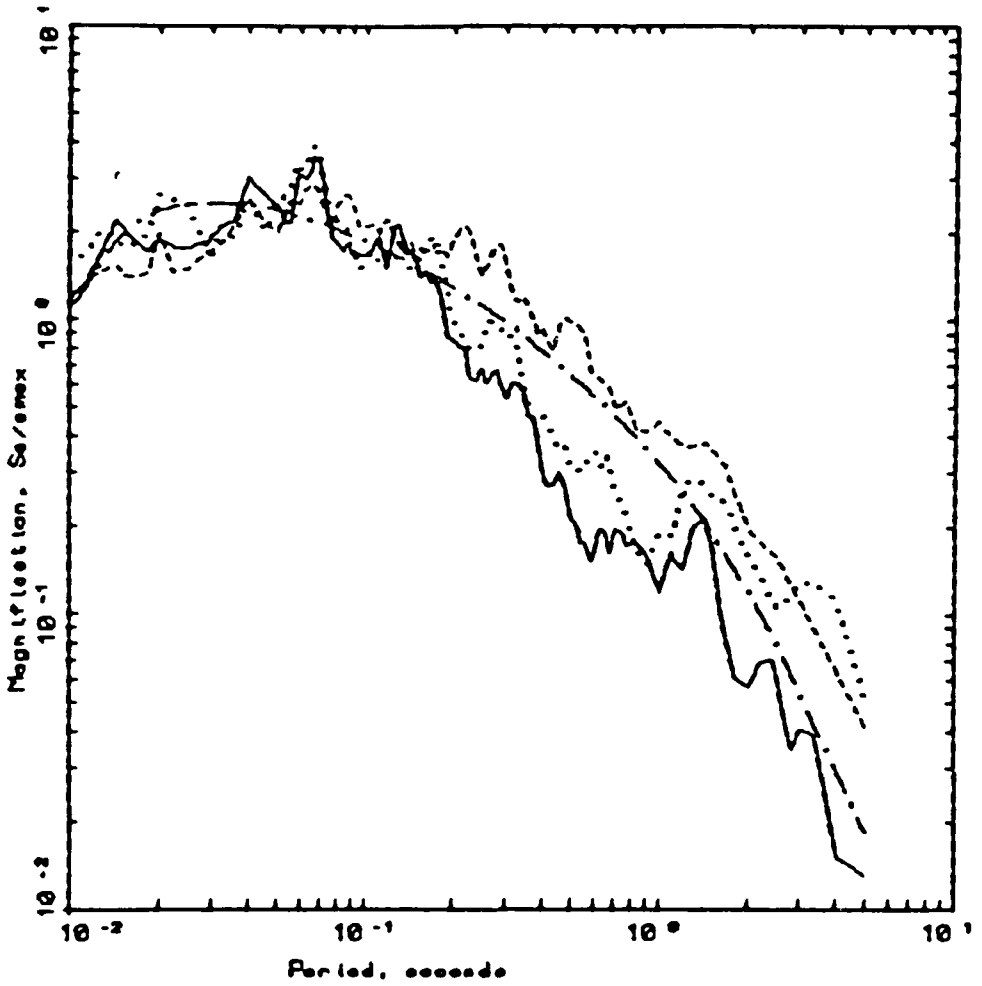

Figure 7 -Comparison of 5% response spectral shapes for the accelerograms in Figure 6. The WES-Rascal RVT estimate is the dashed - dot curve. The BLWN Fourier amplitude spectral estimate combined with the phase of an observed accelerogram is the dashed line (Spectrum 1). The 5% response spectral shapes of the recorded ground accelerations are the solid line (Spectrum 2) and the dotted line (Spectrum 3) for M_w = 6.0 at a distance of 25 km.

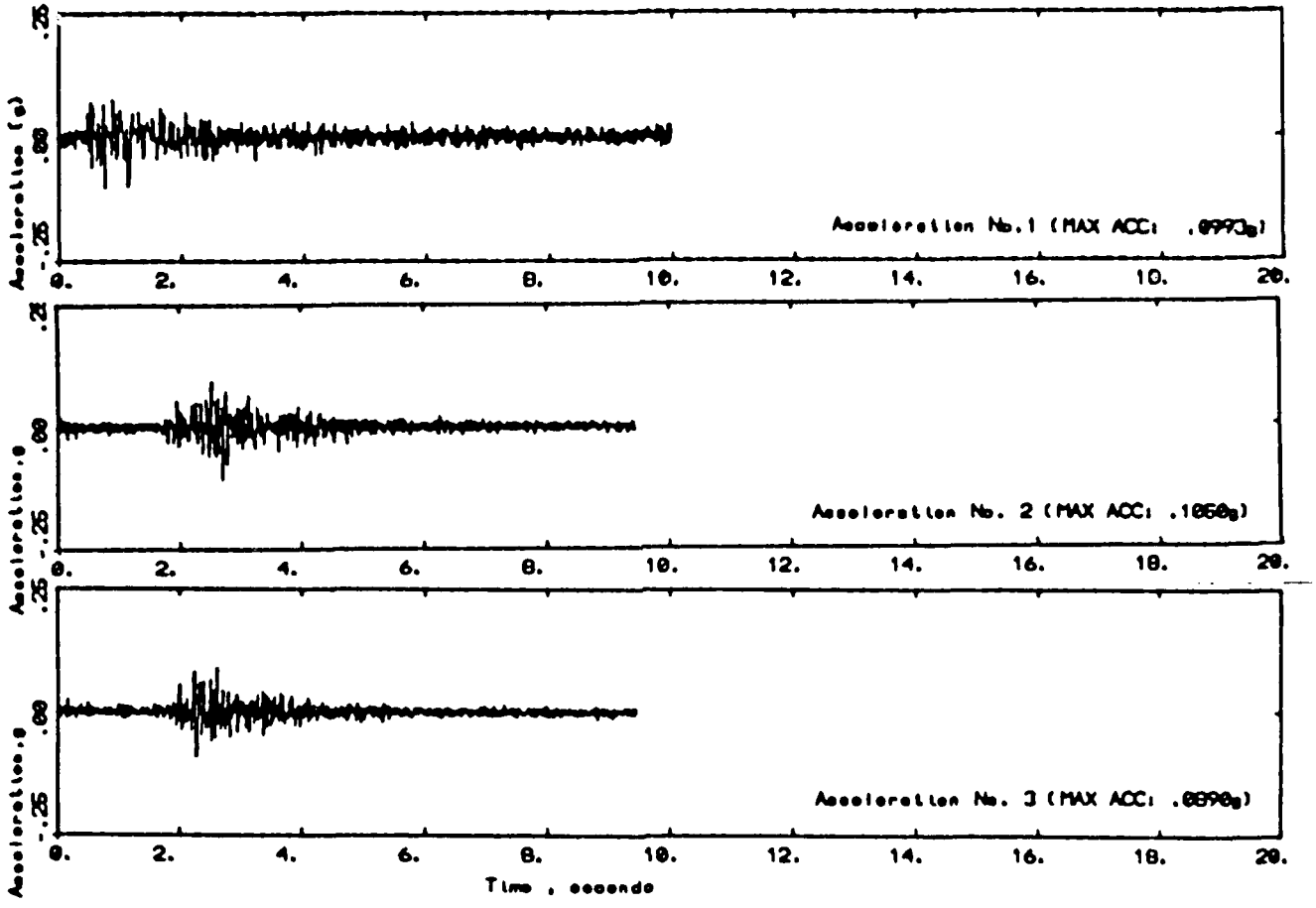

Figure 8 - Comparison of a synthetic accelerogram (Acceleration No. 1) generated as described in Part V to two examples of recorded ground accelerations (Accelerations No. 2 and No. 3) at a distance of 25 km for M_W = 5.3 using ENA parameters (Table 1).

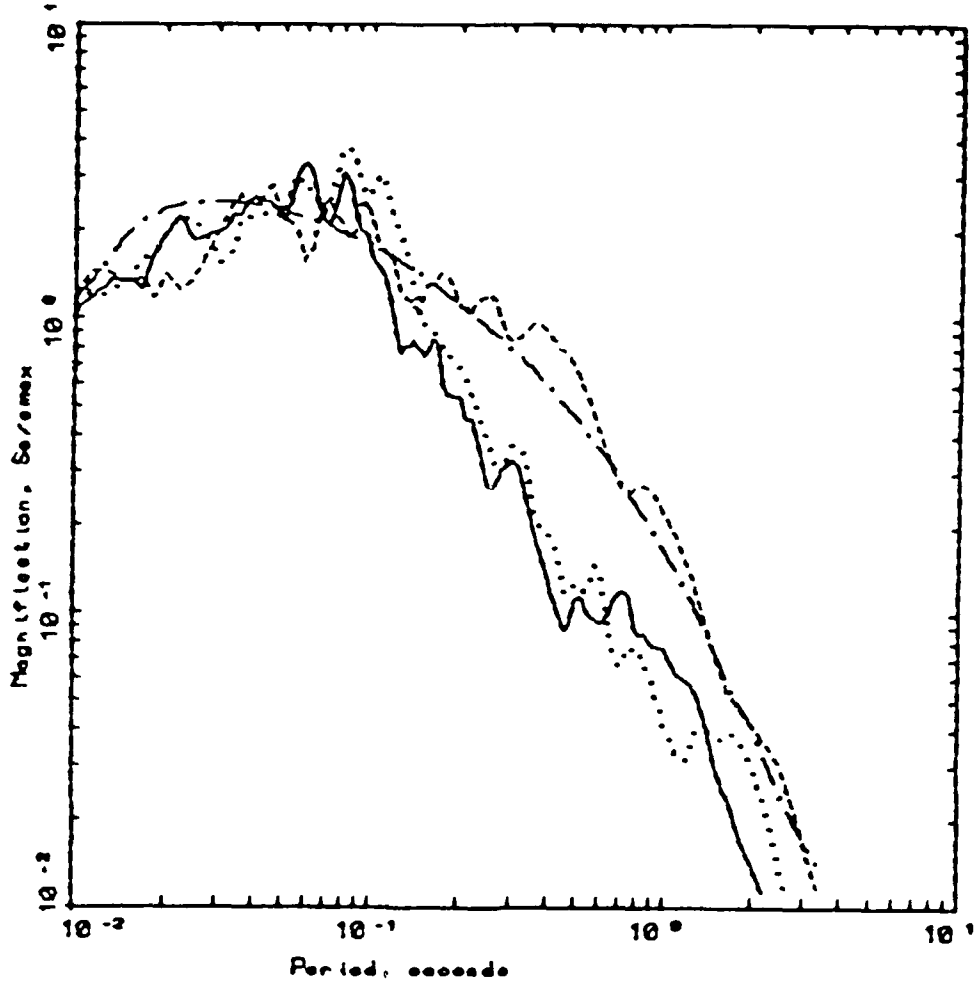

Figure 9 - Comparison of 5% response spectral shapes for the accelerograms in Figure 8. The WES-Rascal RVT estimate is the dashed - dot curve. The BLWN Fourier amplitude spectral estimate combined with the phase of an observed accelerogram is the dashed line (Spectrum 1). The 5% response spectral shapes of the recorded ground accelerations are the solid line (Spectrum 2) and the dotted line (Spectrum 3) for M_w = 5.3 at a distance of 25 km.

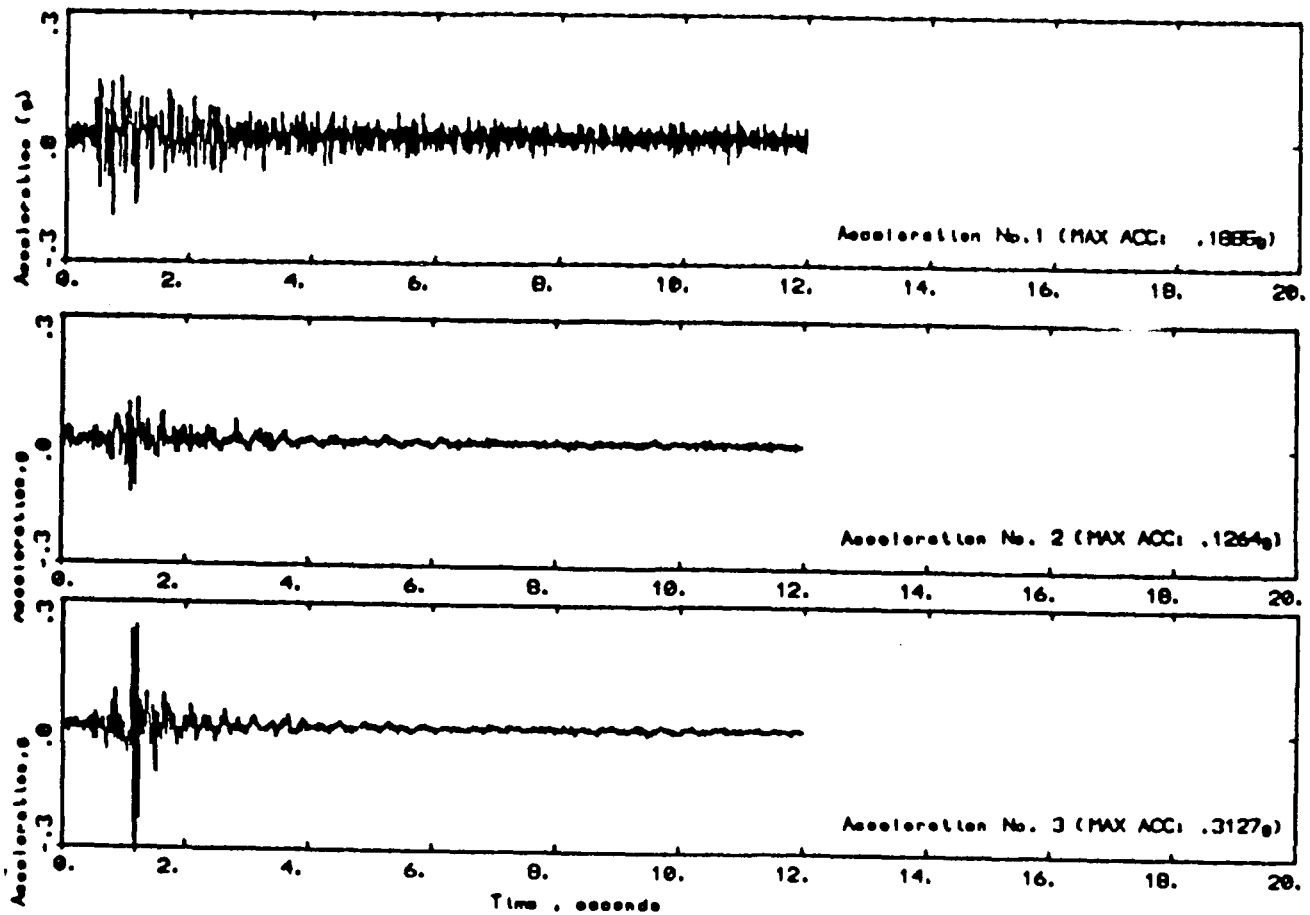

Figure 10 - Comparison of a synthetic accelerogram (Acceleration No. 1) generated as described in Part V to two examples of recorded ground accelerations (Acceleration No. 2 and No. 3) at a distance of 8 km for M_w = 4.5 using ENA parameters (Table 1).

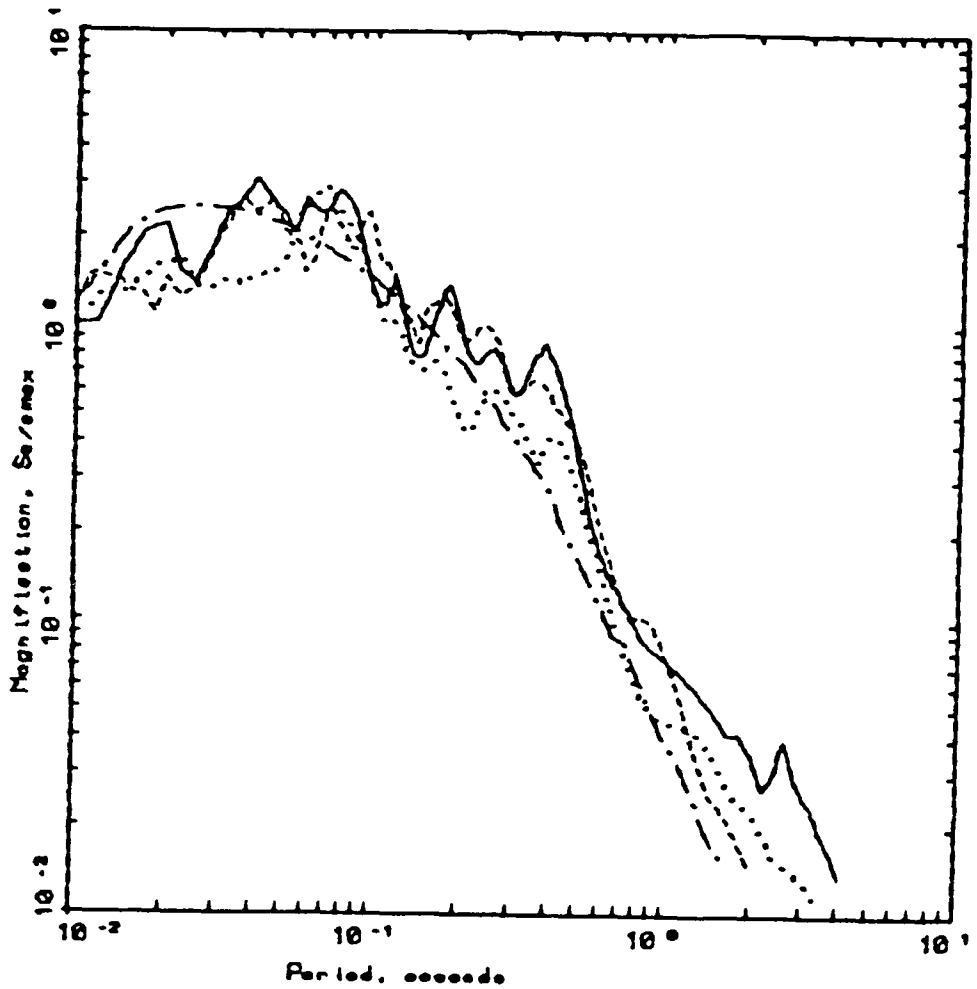

Figure 11 - Comparison of 5% response spectral shapes for the accelerograms in Figure 10. The WES-Rascal RVT estimate is the dashed - dot curves. The BLWN Fourier amplitude spectral estimate combined with the phase of an observed accelerogram is the dashed line (Spectrum 1). The 5% response spectral shapes of the recorded ground accelerations are the solid line (Spectrum 2) and the dotted line (Spectrum 3) for M_w = 4.5 at a distance of 8 km.

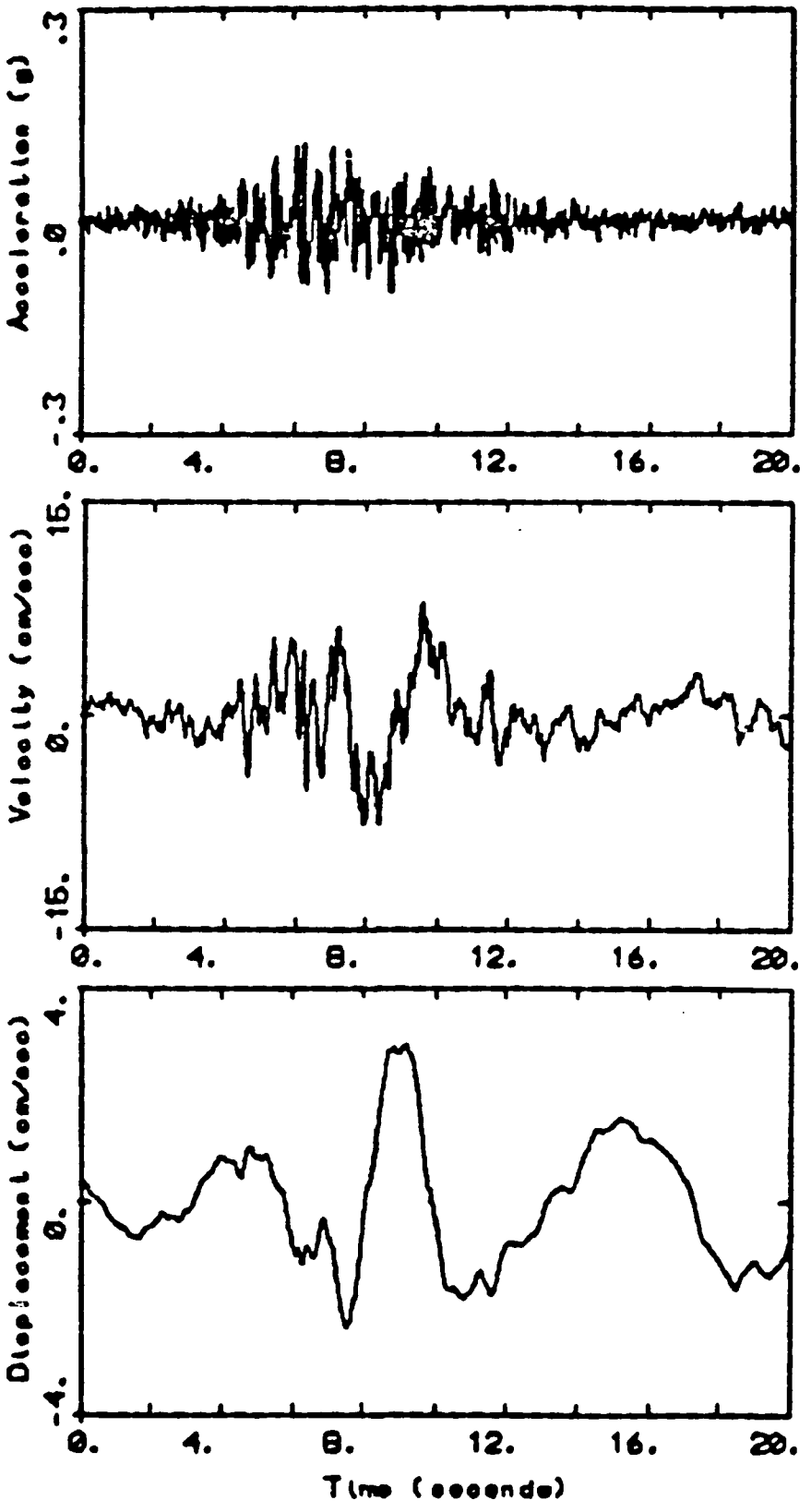

Figure 12 - Synthetic time histories (acceleration, top; velocity, middle; displacement, bottom) generated by adding the phase spectrum from a recorded accelerogram to the BLWN amplitude spectrum for a moment magnitude (M_w) 6.5 earthquake at a distance of 25 km. WNA parameters (Table 1) are used.

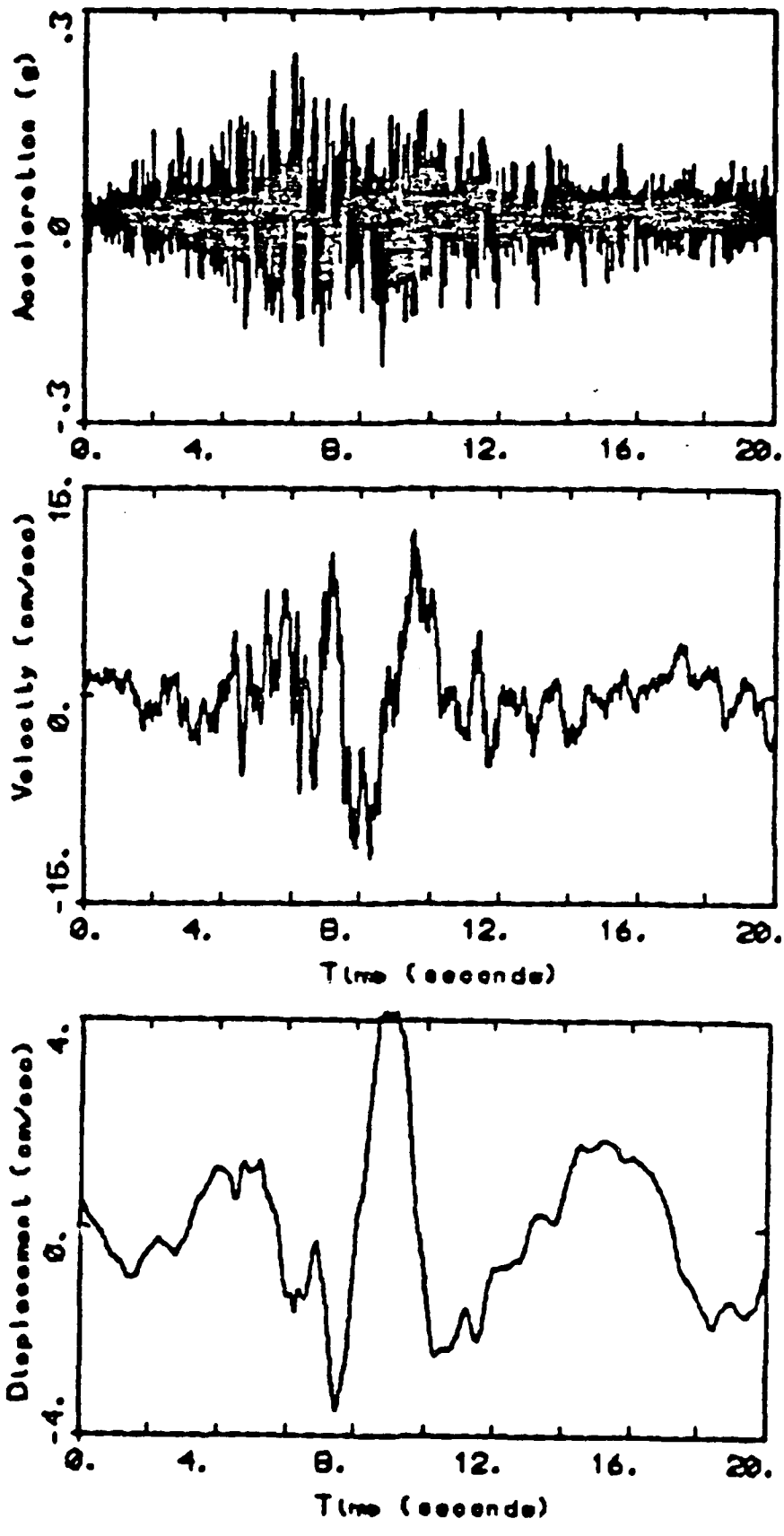

Figure 13 - Synthetic time histories (acceleration, top; velocity, middle; displacement, bottom) generated by adding the phase spectrum from a recorded accelerogram to the BLWN amplitude spectrum for a moment magnitude (M_w) 6.5 earthquake at a distance of 25 km. ENA parameters (Table 1) are used.

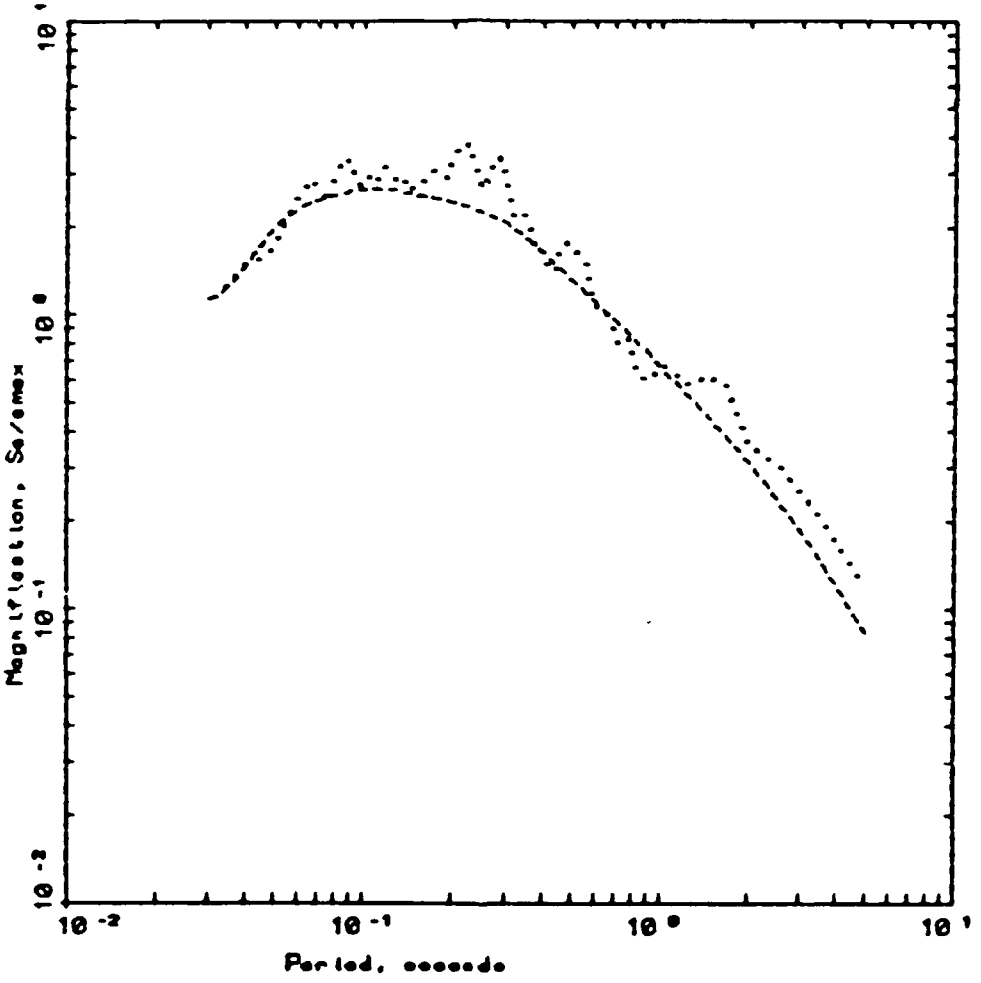

Figure 14 - Comparison of 5% response spectral shape computed from WNA synthetic accelerogram (Figure 12), dashed line, to shape predicted from random vibration theory (RVT) applied to the BLWN amplitude spectrum (Figure 4). In both cases, the Fourier spectral densities are identical.

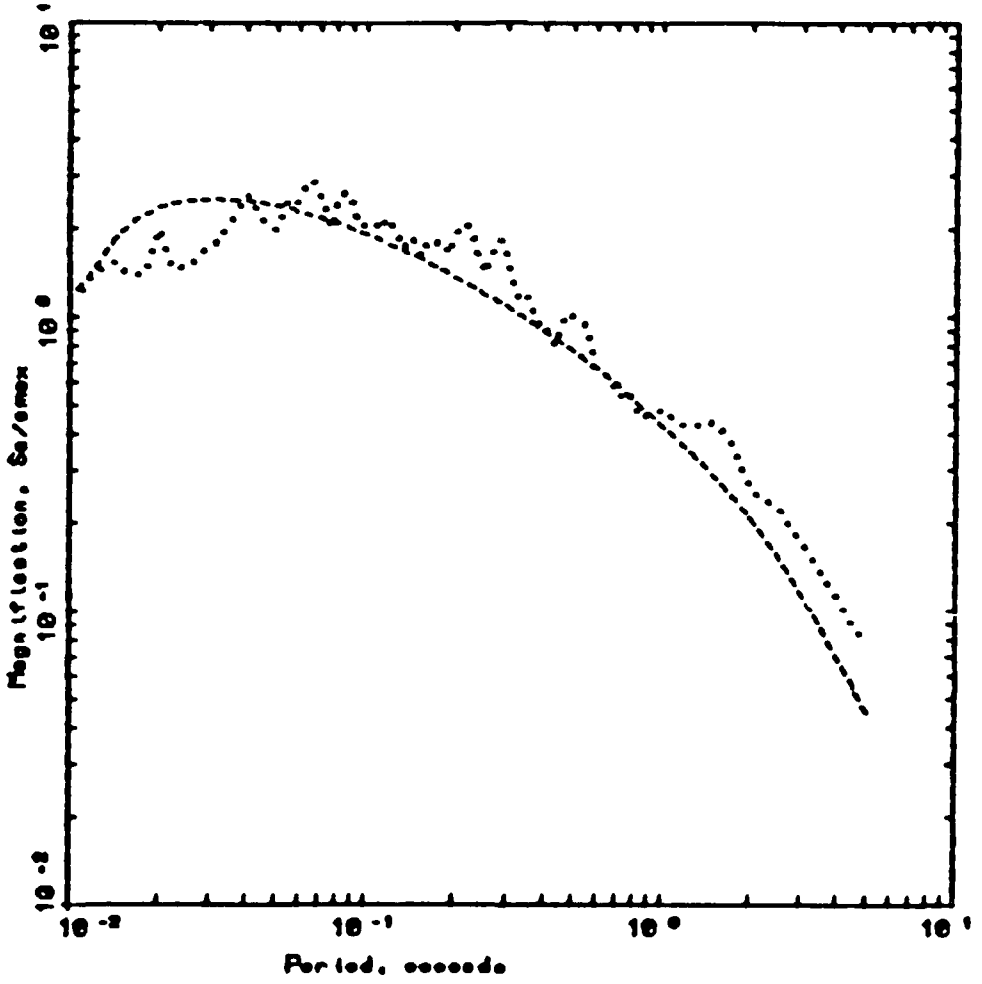

Figure 15 - Comparison of 5% response spectral shape computed from ENA synthetic accelerogram (Figure 13), dashed line, to shape predicted from random vibration theory (RVT) applied to the BLWN amplitude spectrum (Figure 9). In both cases, the Fourier spectral densities are identical.

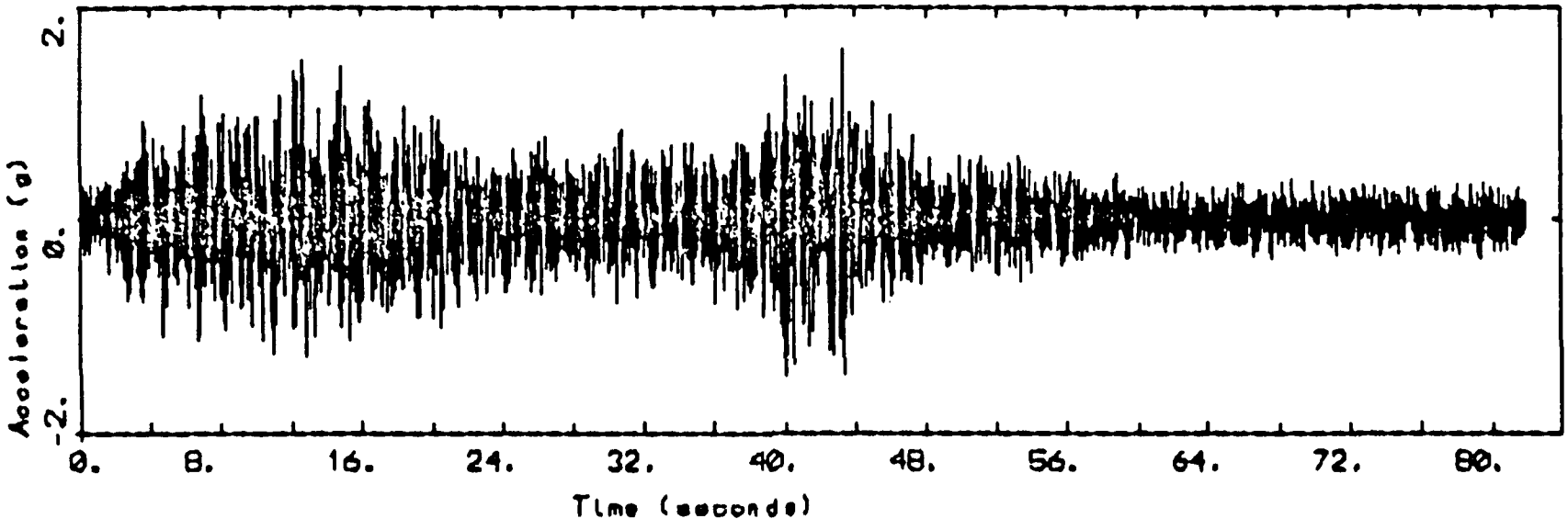

Figure 16 - Synthetic ground acceleration time history for a moment magnitude (M_w) 7.9 earthquake at a focal depth of 10 km and an epicentral distance of 0 km. ENA parameters (Table 1) are used.

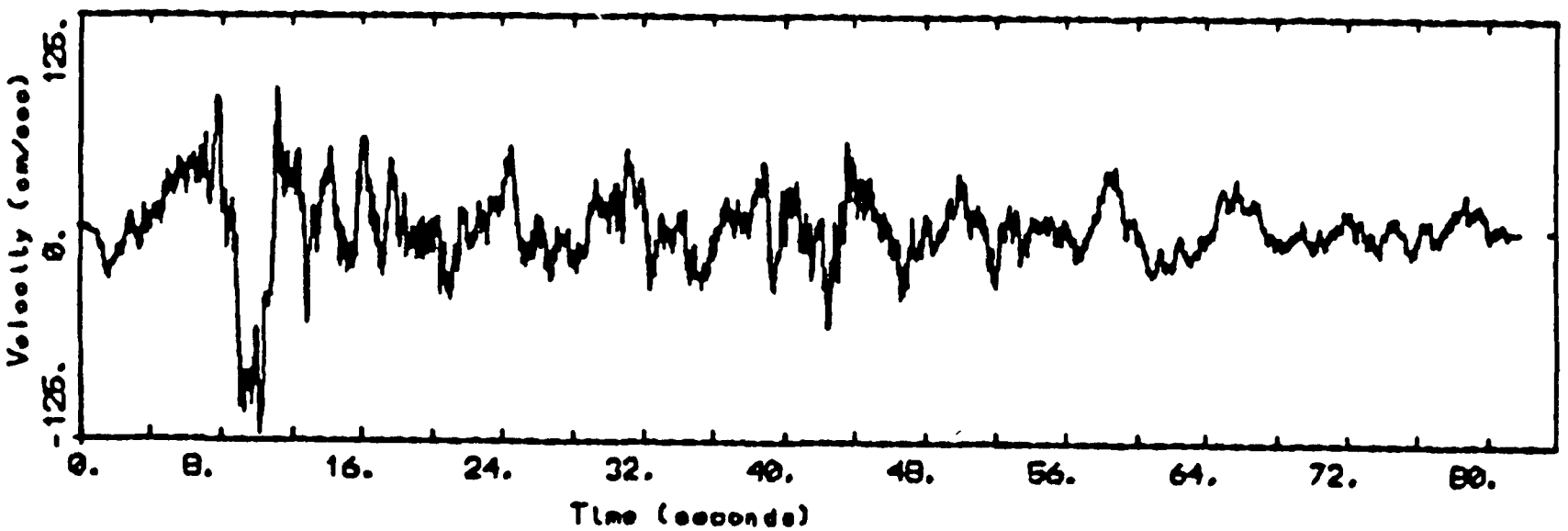

Figure 17 - Synthetic ground velocity time history for a moment magnitude (M_w) 7.9 earthquake at a focal depth of 10 km and an epicentral distance of 0 km. ENA parameters (Table 1) are used.

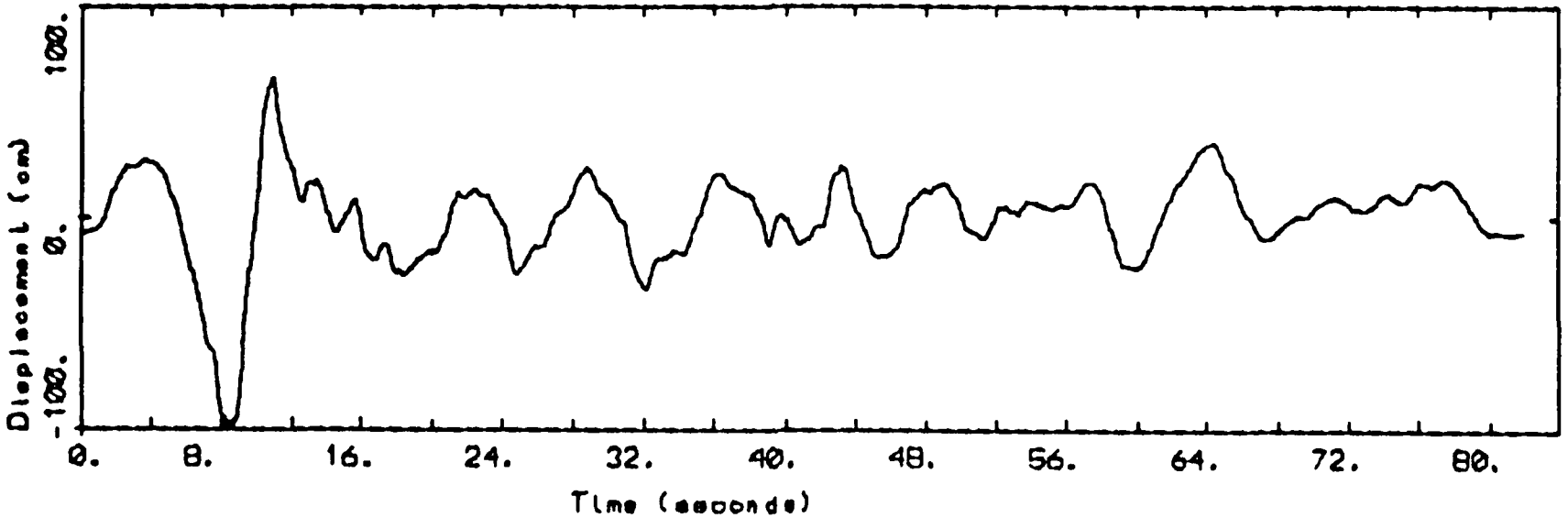

Figure 18 - Synthetic ground displacement time history for a moment magnitude (M_w) 7.9 earthquake at a focal depth of 10 km and an epicentral distance of 0 km. ENA parameters (Table 1) are used.

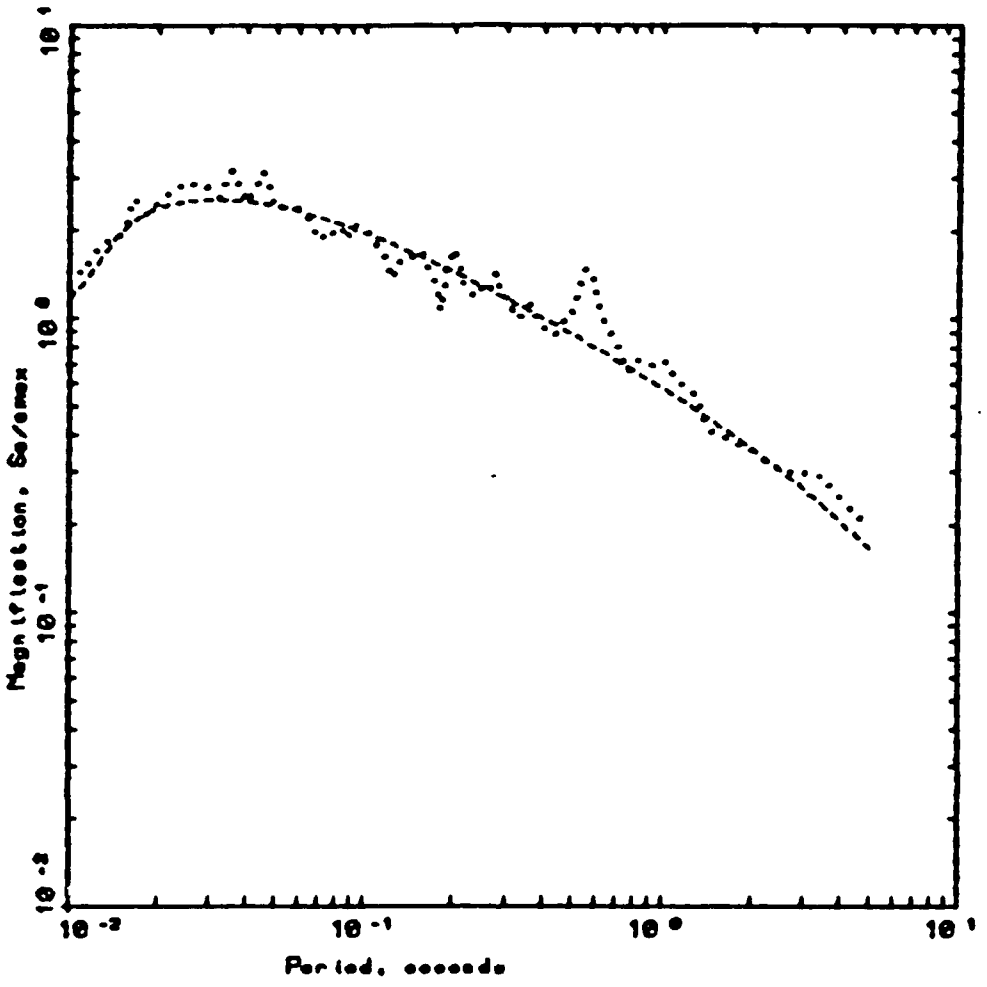

Figure 19 - Comparison of 5% response spectral shape from New Madrid synthetic accelerogram (Figure 16), dashed line, to shape predicted from random vibration theory (RVT) applied to the BLWN amplitude spectrum. In both cases, the Fourier spectral densities are identical.

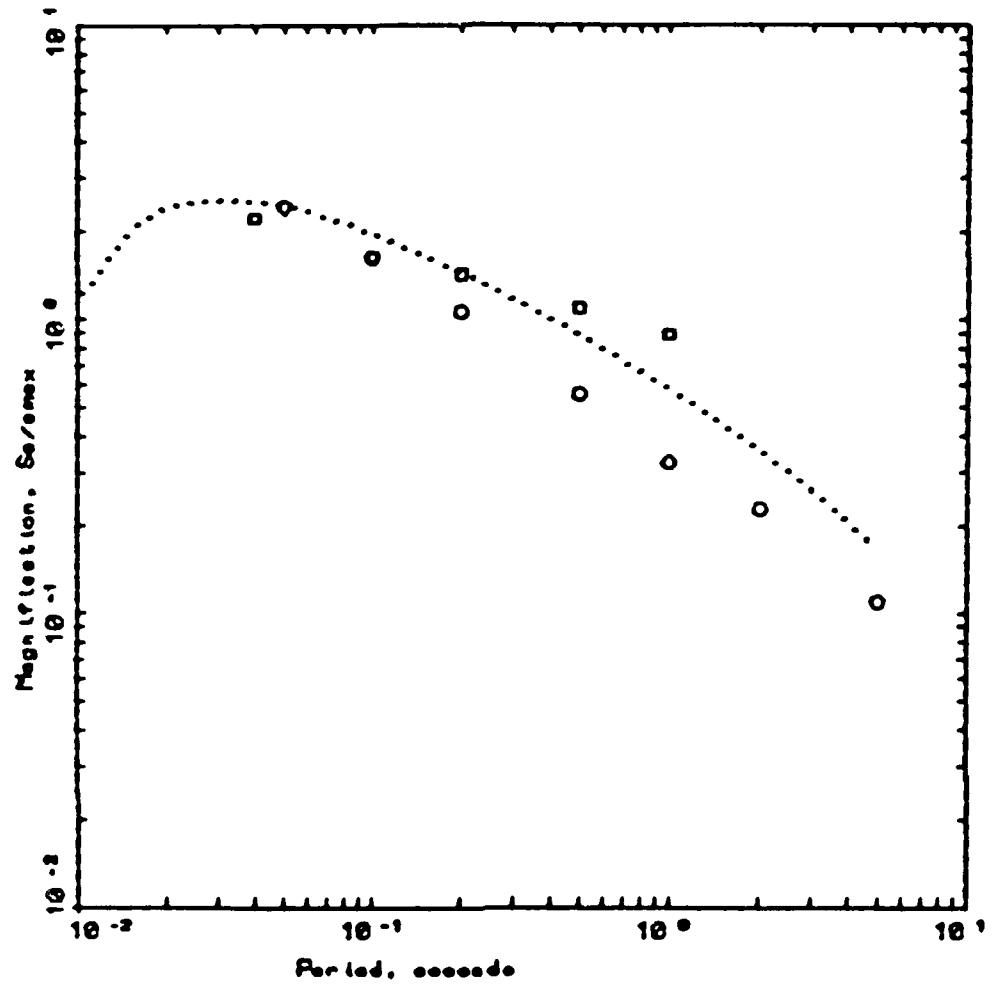

Figure 20 - Comparison of 5% response spectral shape from New Madrid synthetic accelerogram (Figure 16), solid line, to spectral magnifications extrapolated from regression equations of Boore and Atkinson (1987, circles) and Toro et al. (1988, squares). Both of these regression equations are also based on random vibration theory (RVT).

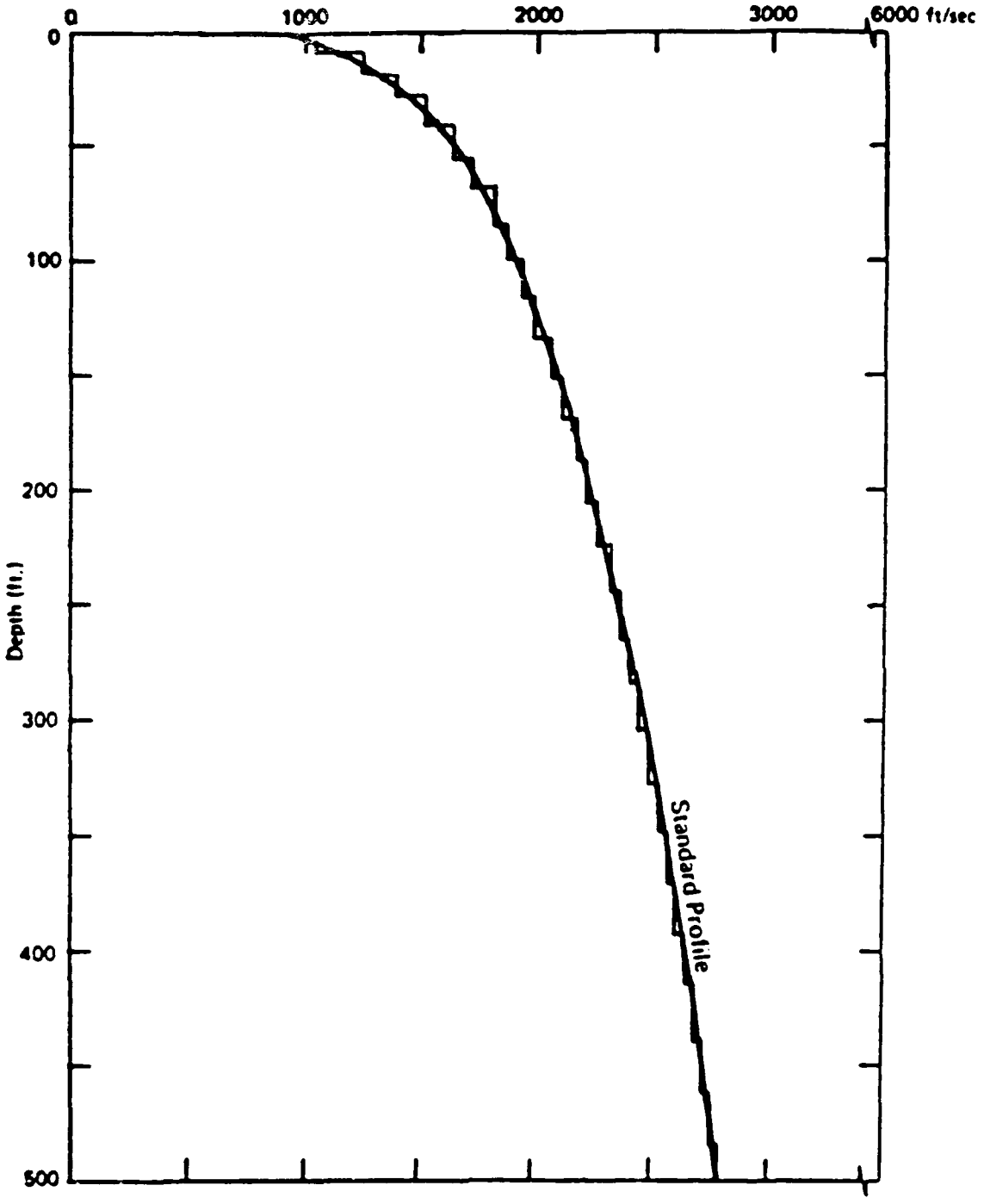

Figure 21 - Generic soil profile appropriate for sand-like Central United States sites.

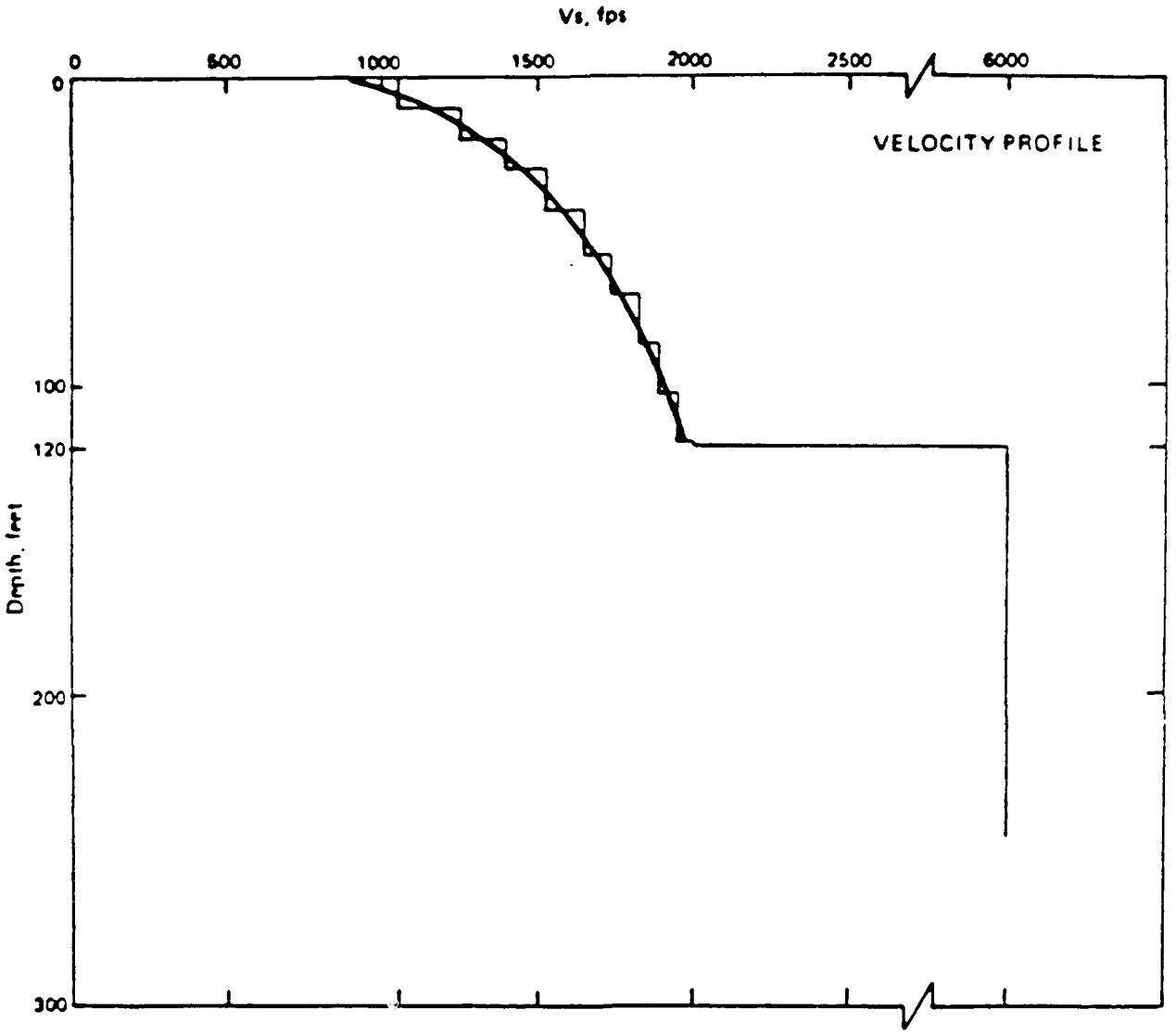

Figure 22 - Soil profiles used in comparison of site response analysis between time domain estimates of peak shear-strain (SHAKE) and random process estimates of peak shear-strain (RASCALS).

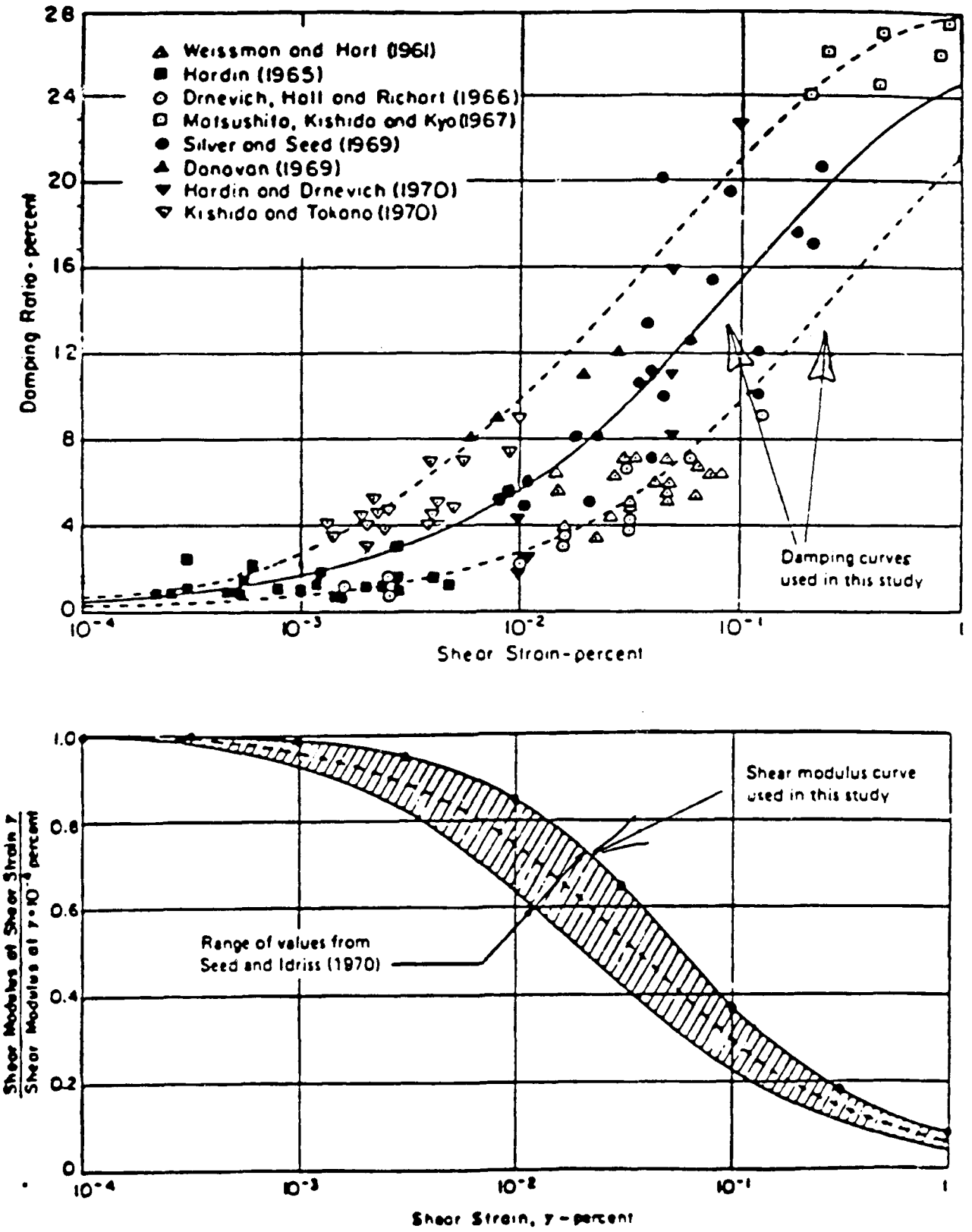

Figure 23 - Plot of shear-strain dependency of shear-wave damping and shear modulus used in all analyses (after Seed and Idriss, 1970).

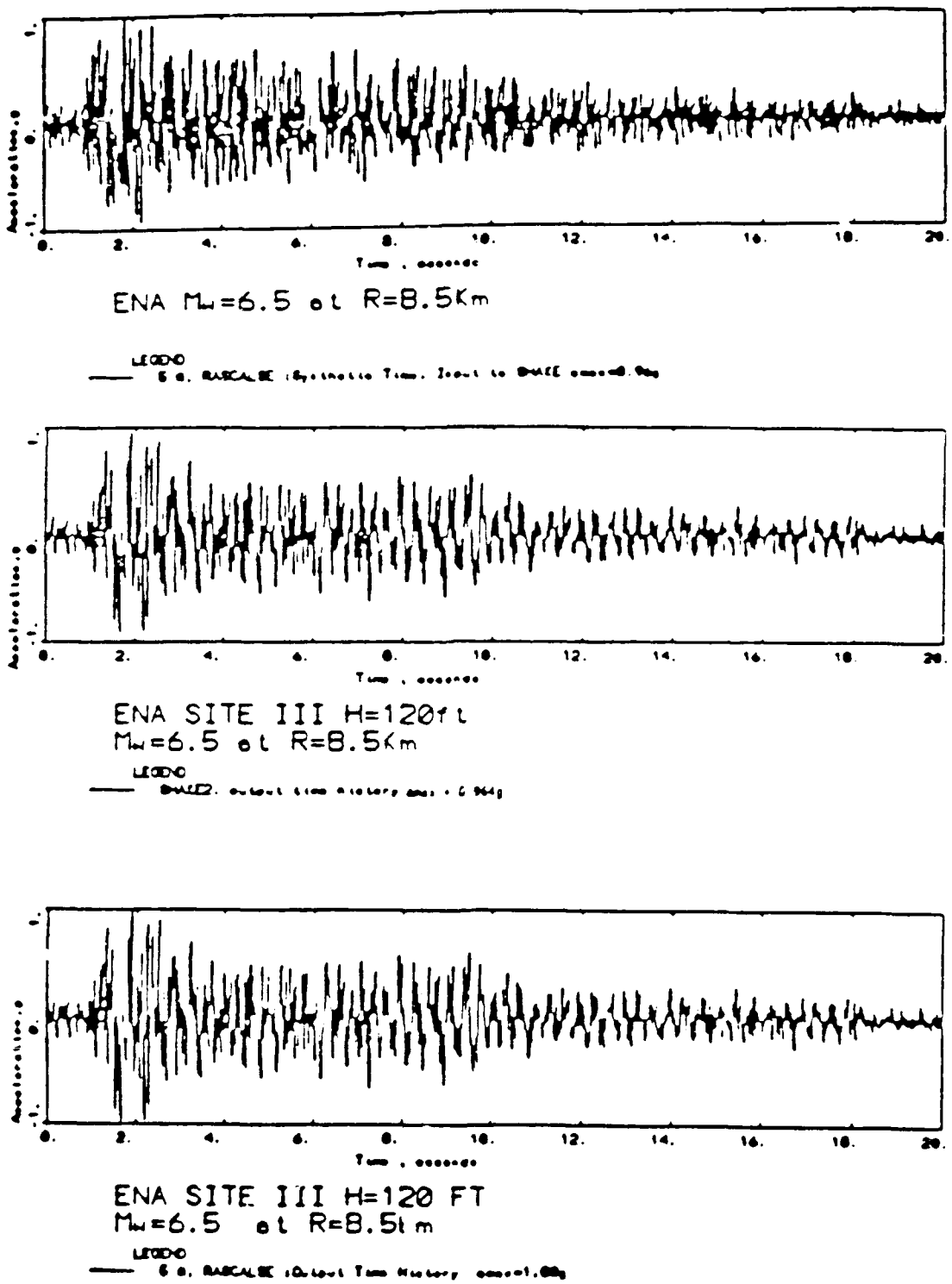

Figure 24 - Plot of synthetics outcrop motion for a M_w = 6.5 event at a hypocentral range of 8.5 km (top trace), output time history resulting from SHAKE analysis (middle trace), and time history resulting from frequency domain random process RASCALS analysis (bottom trace).

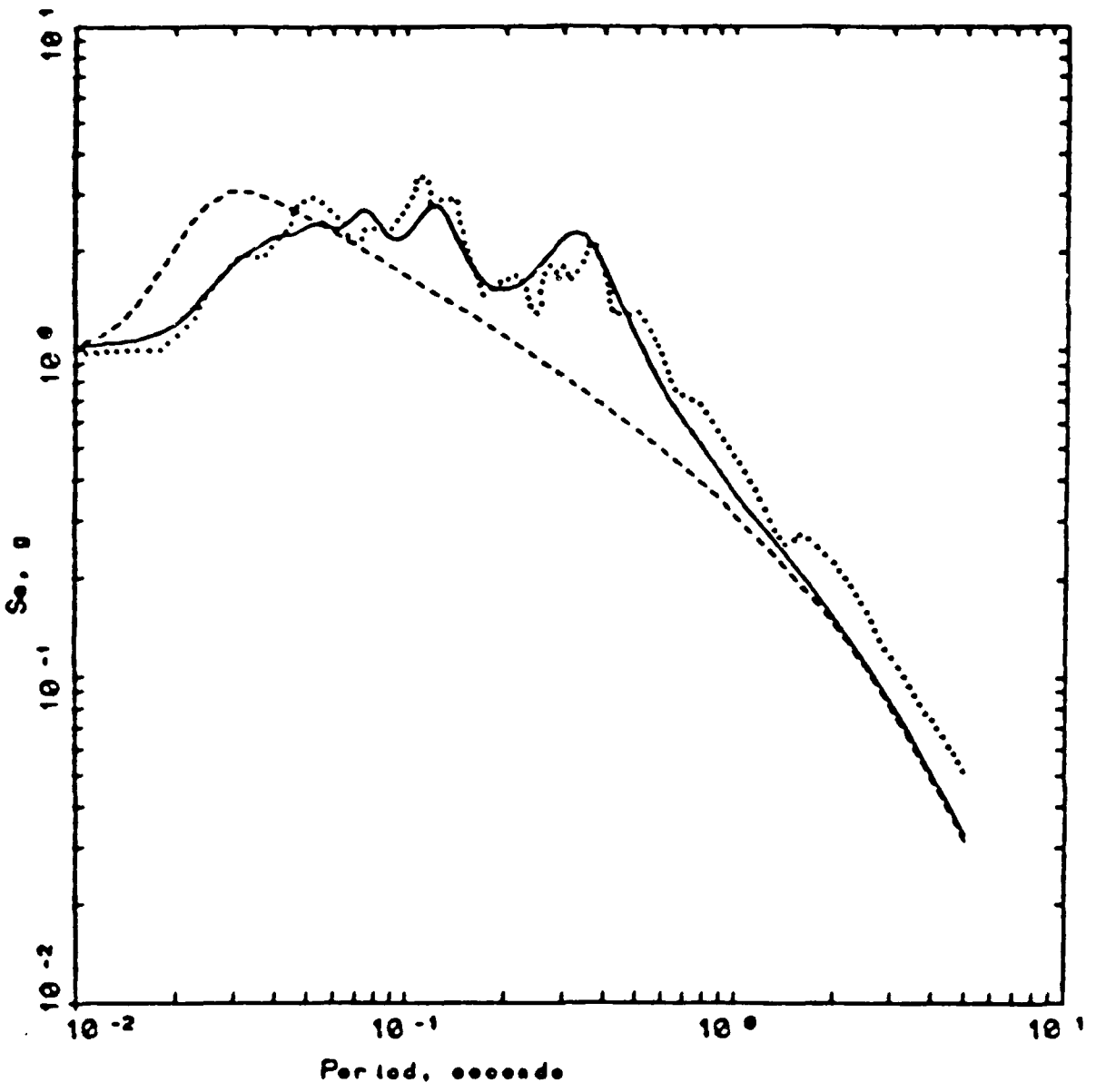

ENA SITE III RESPONSE H=120FT
M_W=6.5 AT R=8.5Km

LEGEND

——— 5 %, RASCALS : RVT (soil) Spectrum amax 1.00g

----- 5 %, RASCALS : RVT (rock) Spectrum amax 1.00g

····· 5 %, SHAKE2: SPECTRUM Site III Response amax=0.964g

Figure 25 - Plot of (5%) absolute acceleration response spectra resulting from the SHAKE site response analysis (dotted line) and random process estimates resulting from RASCALS site response analysis. Also shown is the random process estimates of oscillator response for the rock outcrop (control) motion (dashed line).

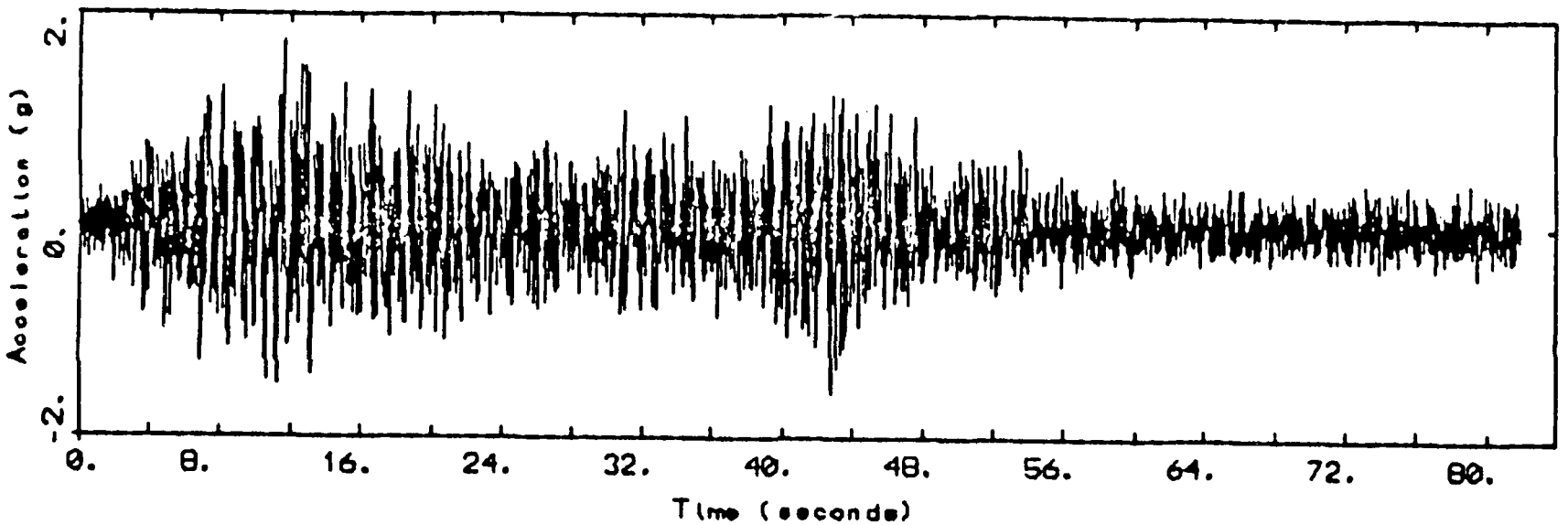

Figure 26 - Synthetic ground acceleration time history for a deep soil profile (Figure 21) resulting from a linear analysis. The control motion is shown in Figure 16 which is the motion predicted for a M_w = 7.9 earthquake at a depth of 10 km and 0 epicentral distance.

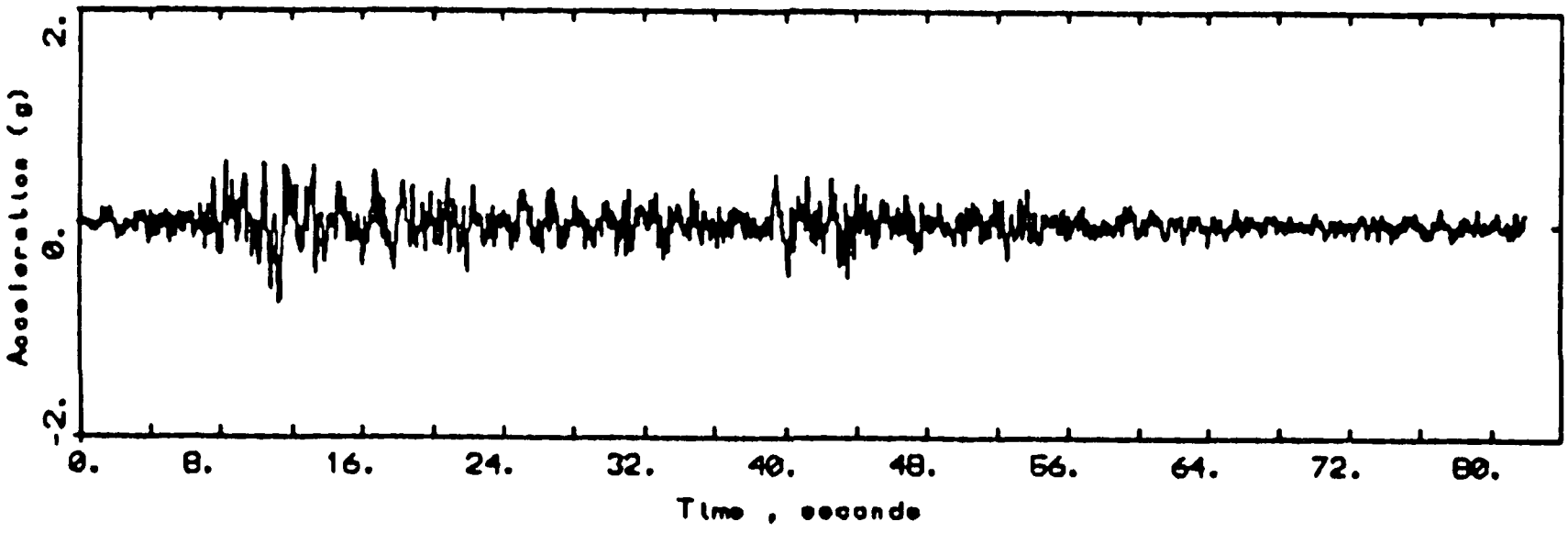

Figure 27 - Synthetic ground acceleration time history for a deep soil profile (Figure 21) resulting from an equivalent-linear analysis using lower range damping (Figure 23). The control motion is shown in Figure 16 which is the motion predicted for a M_w = 7.9 earthquake at a depth of 10 km and 0 epicentral distance.

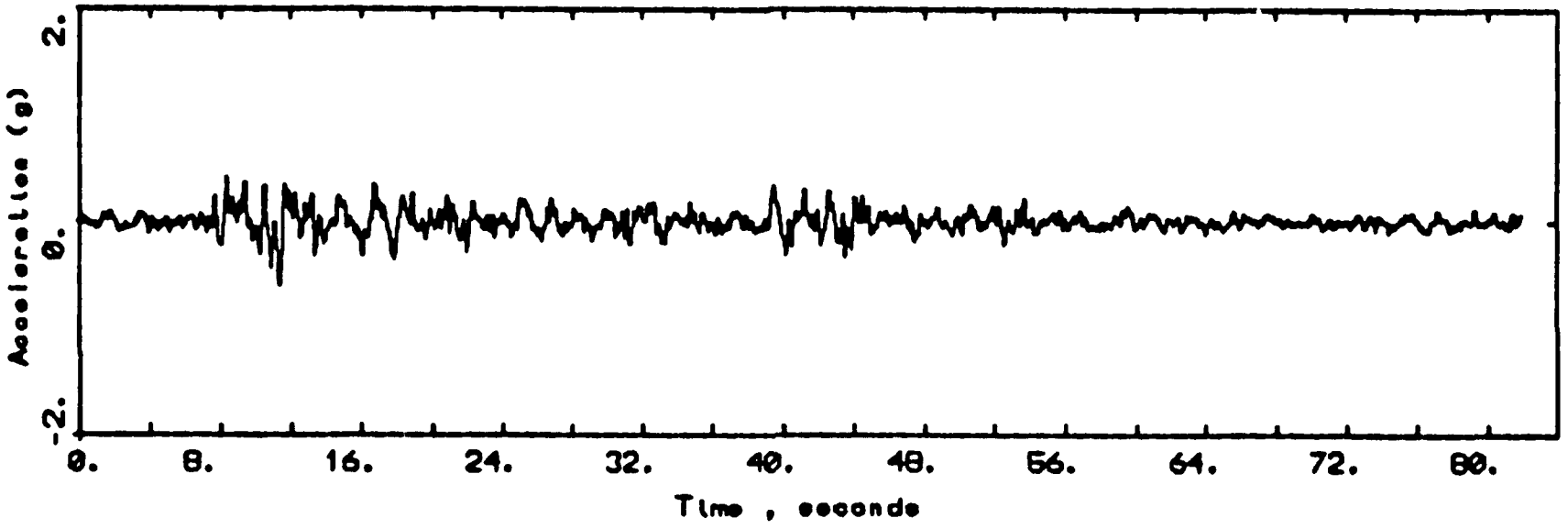

Figure 28 - Synthetic ground acceleration time history for a deep soil profile (Figure 21) resulting from an equivalent-linear analysis using midrange damping (Figure 23). The control motion is shown in Figure 16 which is the motion predicted for a M_w = 7.9 earthquake at a depth of 10 km and 0 epicentral distance.

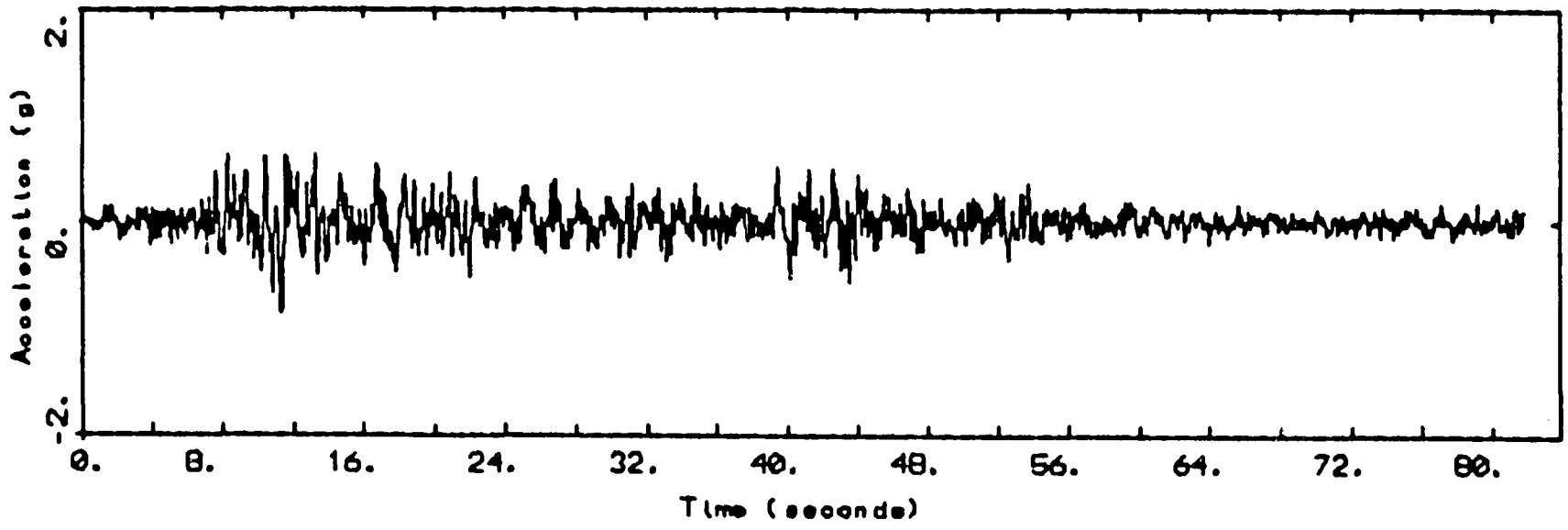

Figure 29 - Synthetic ground acceleration time history for a deep soil profile (Figure 21) resulting from an equivalent-linear analysis using the modulus reduction curve (Figure 23) to model the strain dependency of the initial Qs (small strain) profile. The control motion is shown in Figure 16 which is the motion predicted for a M_w = 7.9 earthquake at a depth of 10 km and 0 epicentral distance.

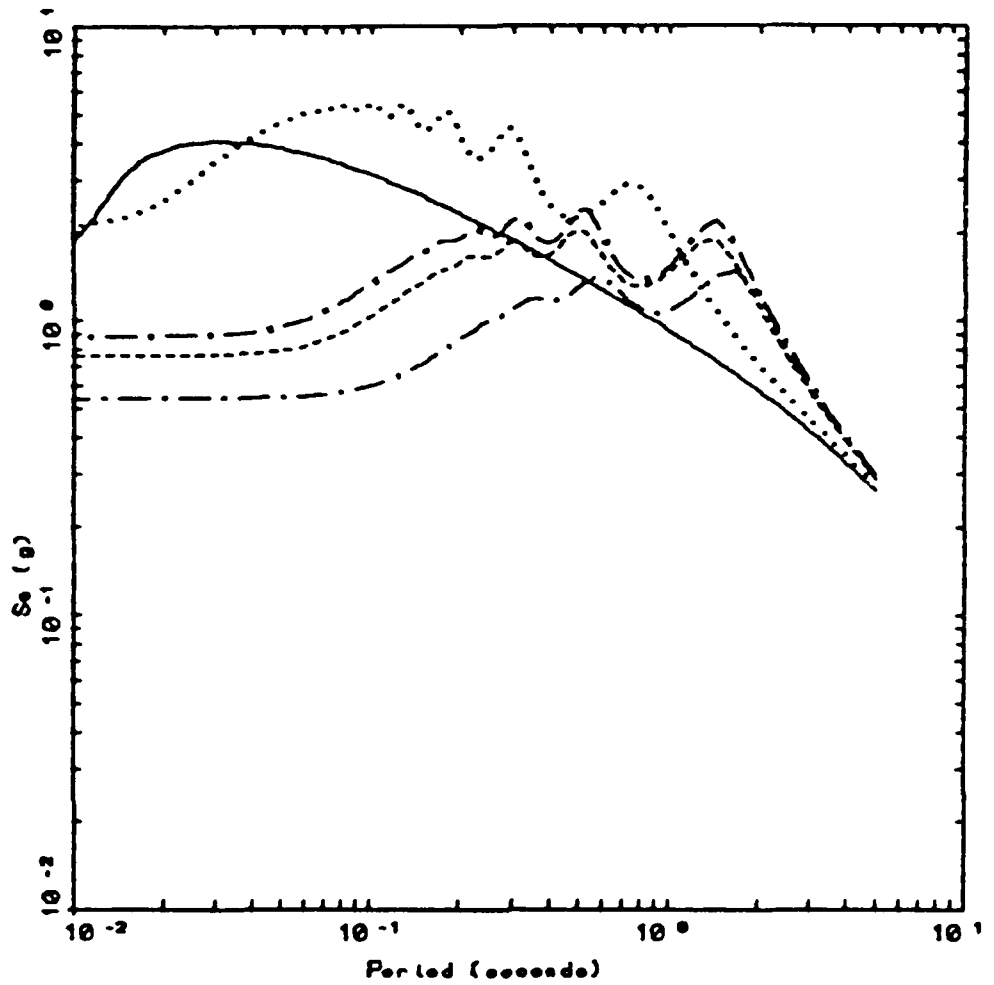

LEGEND

——— 5 %, BLUM RVT OUTCROP MOTION

····· 5 %, BLUM RVT LINEAR SITE RESPONSE

- - - - - 5 %, BLUM RVT LOWER RANGE DAMPING

—·— 5 %, BLUM RVT MID RANGE DAMPING

—·— 5 %, BLUM RVT Q REDUCTION

Figure 30 - Plot of 5% absolute acceleration for the outcrop motion (solid line) as well as for each site response analysis from RVT: Dotted line, linear analysis; Dashed line, equivalent-linear with lower range damping; Dashed-dotted line, equivalent linear with mid-range damping; Dashed-crossed line, equivalent-linear using modulus reduction curve to model strain dependency of initial Qs (small strain) profile.